



COVID-19 Research Tools

Defeat the SARS-CoV-2 Variants

InvivoGen



Dendritic Cell-Specific Disruption of TGF- β Receptor II Leads to Altered Regulatory T Cell Phenotype and Spontaneous Multiorgan Autoimmunity

This information is current as of February 26, 2022.

Rajalakshmy Ramalingam, Claire B. Larmonier, Robert D. Thurston, Monica T. Midura-Kiela, Song Guo Zheng, Faye K. Ghishan and Pawel R. Kiela

J Immunol 2012; 189:3878-3893; Prepublished online 12 September 2012;

doi: 10.4049/jimmunol.1201029

<http://www.jimmunol.org/content/189/8/3878>

Supplementary Material

<http://www.jimmunol.org/content/suppl/2012/09/12/jimmunol.1201029.DC1>

References

This article **cites 47 articles**, 19 of which you can access for free at: <http://www.jimmunol.org/content/189/8/3878.full#ref-list-1>

Why *The JI*? Submit online.

- **Rapid Reviews! 30 days*** from submission to initial decision
- **No Triage!** Every submission reviewed by practicing scientists
- **Fast Publication!** 4 weeks from acceptance to publication

**average*

Subscription

Information about subscribing to *The Journal of Immunology* is online at: <http://jimmunol.org/subscription>

Permissions

Submit copyright permission requests at: <http://www.aai.org/About/Publications/JI/copyright.html>

Email Alerts

Receive free email-alerts when new articles cite this article. Sign up at: <http://jimmunol.org/alerts>



Dendritic Cell-Specific Disruption of TGF- β Receptor II Leads to Altered Regulatory T Cell Phenotype and Spontaneous Multiorgan Autoimmunity

Rajalakshmy Ramalingam,* Claire B. Larmonier,* Robert D. Thurston,*
Monica T. Midura-Kiela,* Song Guo Zheng,[†] Faye K. Ghishan,* and Pawel R. Kiela*[‡]

In vitro data and transgenic mouse models suggest a role for TGF- β signaling in dendritic cells (DCs) to prevent autoimmunity primarily through maintenance of DCs in their immature and tolerogenic state characterized by low expression of MHC class II (MHCII) and costimulatory molecules and increased expression of IDO, among others. To test whether a complete lack of TGF- β signaling in DCs predisposes mice to spontaneous autoimmunity and to verify the mechanisms implicated previously *in vitro*, we generated conditional knockout (KO) mice with Cre-mediated DC-specific deletion of *Tgfb2* (DC-*Tgfb2* KO). DC-*Tgfb2* KO mice die before 15 wk of age with multiorgan autoimmune inflammation and spontaneous activation of T and B cells. Interestingly, there were no significant differences in the expression of MHCII, costimulatory molecules, or IDO in secondary lymphoid organ DCs, although *Tgfb2*-deficient DCs were more proinflammatory *in vitro* and *in vivo*. DC-*Tgfb2* KO showed attenuated Foxp3 expression in regulatory T cells (Tregs) and abnormal expansion of CD25⁺Foxp3⁺ Tregs *in vivo*. *Tgfb2*-deficient DCs secreted elevated levels of IFN- γ and were not capable of directing Ag-specific Treg conversion unless in the presence of anti-IFN- γ blocking Ab. Adoptive transfer of induced Tregs into DC-*Tgfb2* KO mice partially rescued the phenotype. Therefore, *in vivo*, TGF- β signaling in DCs is critical in the control of autoimmunity through both Treg-dependent and -independent mechanisms, but it does not affect MHCII and costimulatory molecule expression. *The Journal of Immunology*, 2012, 189: 3878–3893.

Transforming growth factor- β belongs to a family of evolutionarily conserved molecules with pleiotropic roles in development, carcinogenesis, fibrosis, wound healing, and immune responses (1). In the immune system, TGF- β is critical for the maintenance of peripheral tolerance, an effect believed to be primarily mediated through TGF- β signaling in T cells (1). However, regulation of the innate immune cells, specifically the dendritic cells (DCs), by TGF- β still remains to be characterized in detail. DC maturation induced by TLR ligand/cytokines has been reported to lead to insensitivity to the immunosuppressive effects of TGF- β (2), thus suggesting that loss of TGF- β signaling in DC triggered by inflammation may contribute to the pathogenesis of autoimmune diseases.

In vitro studies using human monocyte-derived DCs (HMDs) or mouse bone marrow-derived DCs (BMDCs) have pointed to a role of TGF- β in maintaining the immature state of DCs, with low expression of MHC class II (MHCII) and costimulatory molecules, and low IL-12 production in response to LPS, TNF- α , or IL-1 stimulation (3–5). In addition to preventing the maturation of DCs, TGF- β also suppresses DC E-cadherin expression, a recently described hallmark of mucosal inflammatory DCs (6). It has also been shown to affect chemotactic responses in DCs by inhibiting the expression of CCR7 in murine or human DCs (7) and by increasing the expression of CCR-1, CCR-3, CCR-5, CCR-6, and CXCR-4 in immature HMDs (8). Autocrine action of TGF- β has also been shown to sustain the activation of IDO in DCs and to maintain their tolerogenic function (9, 10).

However, there is very limited literature confirming these mechanisms *in vivo*. Mice deficient in Runx3, a transcription factor expressed in leukocytes, including DCs, which functions as part of the TGF- β signaling cascade, develop allergic airway inflammation, spontaneous colitis, and a late-onset progressive hyperplasia of the glandular mucosa of the stomach, and maturation of Runx3^{-/-} DCs is accelerated and accompanied by increased efficacy to stimulate T cells (11, 12). Transgenic mouse model with partial attenuation of TGF- β signaling in CD11c⁺ DCs and NK cells (CD11c^{dnR} mice) showed increased susceptibility to experimental autoimmune encephalomyelitis when crossed with Mog^{TCR} transgenic mice (13). However, when unchallenged, these mice did not show any signs of autoimmunity (14). Moreover, expression of dominant negative TGF β RII driven by 5.5 kb of the CD11c gene promoter profoundly affected NK cell homeostasis, NK production of IFN- γ , and the NK cell response to parasitic infection (15). More recently, Boomershteyn et al. (16) attempted the deletion of *Tgfb2* in fibroblasts with Cre expression driven by *S100A4* gene promoter and observed autoimmune pancreatitis, which was ultimately attributed to the leaky Cre expression in DCs. Collectively,

*Department of Pediatrics, Steele Children's Research Center, University of Arizona, Tucson, AZ 85724; [†]Division of Rheumatology and Immunology, Department of Medicine, Keck School of Medicine, University of Southern California, Los Angeles, CA 90033; and [‡]Department of Immunobiology, University of Arizona, Tucson, AZ 85724

Received for publication April 6, 2012. Accepted for publication August 11, 2012.

This work was supported by National Institutes of Health Grant 5R01DK067286 (to P.R.K.) and a Dorrance Foundation fellowship (to R.R.).

The microarray data presented in this article have been submitted to the Gene Expression Omnibus (<http://www.ncbi.nlm.nih.gov/geo/>) under accession number GSE39651.

Address correspondence and reprint requests to Dr. Pawel R. Kiela, Assoc. Prof. of Pediatrics and Immunobiology, Steele Children's Research Center, Arizona Health Sciences Center 6341E, University of Arizona, Tucson, AZ 85724. E-mail address: pkiela@peds.arizona.edu

The online version of this article contains supplemental material.

Abbreviations used in this article: B6, C57BL/6J; BM, bone marrow; BMDC, bone marrow-derived dendritic cell; CM, complete medium; Ct, threshold cycle; DC, dendritic cell; Flt3L, Flt3 ligand; HMD, human monocyte-derived dendritic cell; iTreg, induced regulatory T cell; KO, knockout; LN, lymph node; MHCII, MHC class II; MLN, mesenteric lymph node; pDC, plasmacytoid dendritic cell; qPCR, quantitative PCR; SP, single-positive; TBP, TATA box binding protein; Treg, regulatory T cell.

Copyright © 2012 by The American Association of Immunologists, Inc. 0022-1767/12/\$16.00

the models used to date have not been able to conclusively and definitively address the role of TGF- β signaling in DCs in vivo.

An important aspect of DC-mediated tolerance requires their functional interaction with regulatory T cells (Tregs), immunosuppressive cells that play a dominant role in maintaining tolerance to self-Ags. One of the mechanisms by which Tregs exert their immunosuppressive function relies on their ability to modulate DC function. Tregs not only downmodulate the expression of costimulatory molecules such as CD80/CD86 on DCs but also induce a tolerogenic phenotype (17). DCs are also involved in Treg homeostasis, and a feedback loop between the numbers of DCs and Tregs in vivo has been postulated as crucial for the balance between immunity and tolerance (18). In addition, DCs also actively induce Foxp3⁺ Tregs from naive T cell precursors in the presence of TGF- β (19). However, although the direct effect of TGF- β on T cells in this process has been well documented, the role of TGF- β signaling in DCs to maintain Treg homeostasis and differentiation has not been examined in detail.

To assess the in vivo significance of TGF- β signaling in DCs in a more comprehensive fashion, we developed a conditional knockout (KO) mouse model (DC-*Tgfb2* KO) by crossing DC-specific Cre deleter mouse strain (20) with mice having exon 2 of *Tgfb2* gene flanked by loxP sites (21). CD11c-Cre mice are BAC transgenics in which Cre recombinase replaced CD11c exon I in the entire *Itgax* (CD11c) gene, which lacks the 5' end of the adjacent *Itgam* (CD11b) gene, thus preventing the overexpression of the latter (20). DC-*Tgfb2* KO mice die by 14 wk of age with multiorgan autoimmune inflammation. Despite no difference in

MHCII and costimulatory molecule expression, *Tgfb2*-deficient DCs were more proinflammatory and less immunosuppressive as evidenced in the adoptive DC and T cell cotransfer studies. We observed decreased number of CD25⁺Foxp3⁺ peripheral Tregs with concomitant expansion of CD25⁻Foxp3⁺ cells, as well as increased numbers of activated effector T cells in DC-*Tgfb2* KO mice. The DCs from the KO mice were unable to direct Ag-specific induced Treg (iTreg) differentiation because of elevated IFN- γ production. These findings reveal the importance of TGF- β signaling in DCs in preserving both DC and Treg function, independently of Ag presentation or costimulation.

Materials and Methods

Mice

B6.129S6-*Tgfb2*^{tm1Hlm} mice, carrying homozygous loxP site insertion flanking exon 2 of *Tgfb2* gene (21) were obtained from National Cancer Institute (Frederick, MD) mouse repository (strain 01XN5). CD11c-Cre transgenic mice (B6.Cg-Tg(*Itgax*-cre)1-1Reiz/J) (20), OT-II transgenic mice (B6.Cg-Tg(*Tcr*aTcrb)425Cbn/J), *Rag1*^{-/-} (B6.129S7-*Rag1*^{tm1Mom/J}) (22), and wild-type C57BL/6J (B6) were obtained from The Jackson Laboratory. All mice were maintained in a conventional animal facility at the University of Arizona. A separate colony of Cre⁻ and DC-*Tgfb2* KO was established and maintained in an ultraclean (*Helicobacter* sp.-free) facility through embryo transfer. All animal experiments were approved by the University of Arizona Institutional Animal Care and Use committee.

Polymerase chain reaction

Cre-mediated recombination in T cells and BMDCs was tested using PCR with primers specifically designed to span exon 2 of *Tgfb2* gene. DNA was

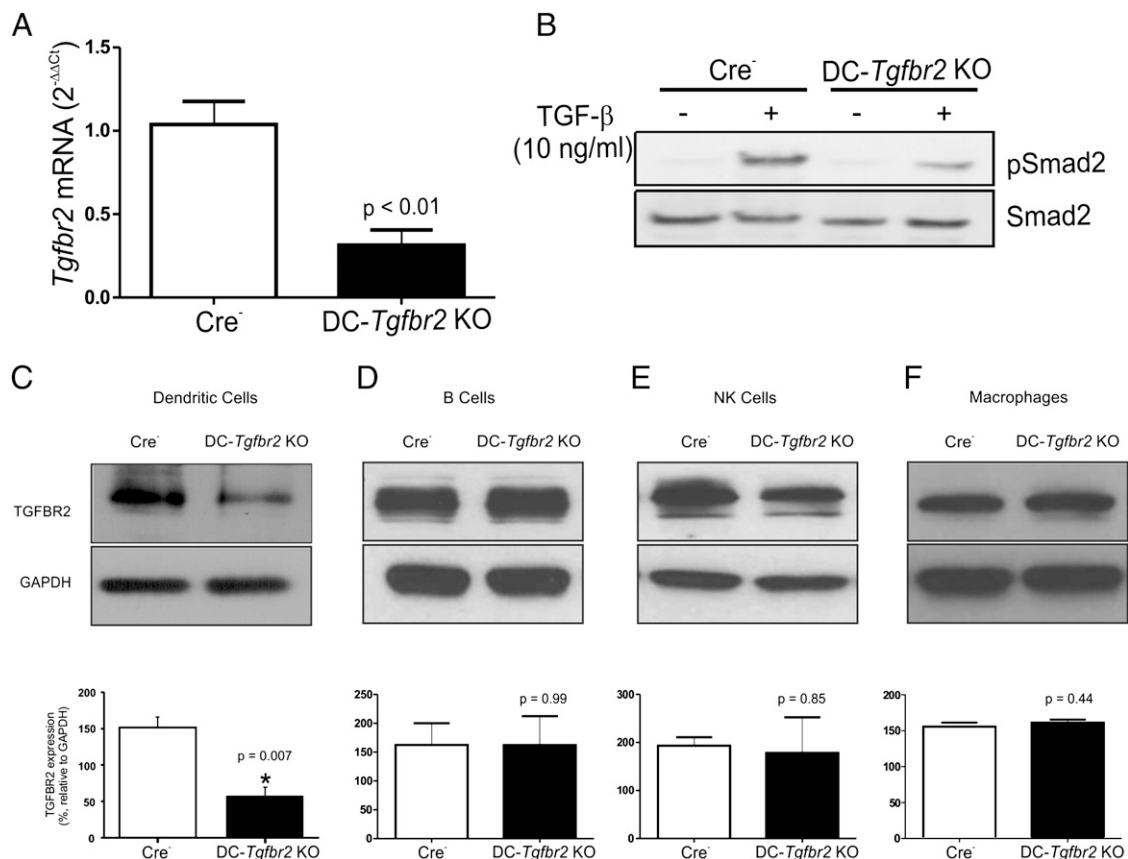


FIGURE 1. Efficiency of *Tgfb2* deletion in DCs. (A) mRNA expression of *Tgfb2* in BMDCs from control Cre⁻ and DC-*Tgfb2* KO mice. Each sample was normalized to TBP expression. Bars represent means and SEM of samples from five individual mice; (B) CD11c⁺ BMDCs were stimulated with TGF- β (10 ng/ml) for 30 min, and pSmad2 expression was determined by Western blotting (representative results of three different experiments); (C–F) TGFBR2 protein expression was analyzed by Western blotting in protein lysates from magnetically sorted splenic CD11c⁺ DCs (C), CD19⁺ B cells (D), DX5⁺ NK cells (E), and resident peritoneal macrophages (F) of Cre⁻ and DC-*Tgfb2* KO mice. GAPDH is shown as a loading control. Corresponding densitometric analysis of Western blots relative to GAPDH are presented in the bottom panels. All *p* values were obtained using a Student *t* test.

extracted from cells using the DNA isolation kit from Qiagen (Valencia, CA) and subjected to PCR amplification. Each PCR mixture contained 50–100 ng DNA, 5 μ l 10 \times AccuPrime Reaction mix (Life Technologies, Grand Island, NY), 0.5 μ l 10 μ M gene-specific forward and reverse primers, 0.4 μ l AccuPrime DNA polymerase (Life Technologies), and water to 50 μ l. Primers used for exon 2 were 5'-GAGAGGGTATACTCTCCATC-3' (forward) and 5'-GTGGATGGATGGTCTCTATTAC-3' (reverse) and for exon 5 were 5'-TAGCCACACAGCCATCTCTCA-3' (forward) and 5'-TGGATGGATGCATCTTTCTGG-3' (reverse).

Generation of BMDCs

BMDCs were prepared as described previously (23). Briefly, BM cells were suspended in complete RPMI 1640 medium supplemented with 10% heat-inactivated FBS (Hyclone, Thermo Scientific, Rockford, IL), 50 mM 2-ME, 100 U/ml penicillin, 100 μ g/ml streptomycin, and 5 mM glutamine (complete medium [CM]). For GM-CSF/IL-4-DC culture, BM cells were resuspended at 1.5×10^6 /ml in CM containing 10 ng/ml GM-CSF and 10 ng/ml IL-4 (PeproTech, Rocky Hill, NJ) and seeded at 3 ml/well in 6-well tissue culture plates. At days 3 and 5, half the medium was removed and fresh medium with cytokines was added to the cells. For Flt3L ligand (Flt3L)-DC culture, BM cells were resuspended at 1×10^6 cells/ml in CM containing 100 ng/ml human recombinant Flt3L (Cell Signaling Technology, Danvers, MA) and seeded at 3 ml/well in 6-well tissue culture plates. At day 6 for GM-CSF/IL-4 DC or day 8 for Flt3L DC, loosely adherent cells were collected and CD11c⁺ cells were purified by magnetic selection using CD11c⁺ microbeads (Miltenyi Biotec, Auburn, CA). Cells were then replated at 1×10^6 cells/ml in CM. Maturation of the DCs was induced by adding LPS (Calbiochem, EMD Millipore, Billerica, MA) at 100 ng/ml. All cells were incubated at 37°C with 10% CO₂.

Flow cytometry

Single-cell suspensions were prepared from the thymus, spleen, and mesenteric lymph nodes (MLNs) and subjected to red cell lysis. After blocking for 15 min with anti CD16/CD32 Ab, the cells were labeled with fluorescent conjugated Abs and incubated for 30 min at 4°C. Samples were analyzed using FACS-

Calibur, and data were analyzed using FlowJo software (Tree Star, Ashland, OR). Anti-mouse CD11c-allophycocyanin/PE, CD3-Percp, MHCII-FITC, CD80-allophycocyanin, CD86-allophycocyanin, CD40-FITC/PE, CCR7-PE, CD11b-PE, CD8a-FITC/allophycocyanin/Percp, CD4-PE/FITC, CD24-PE-Cy7, Qa-2-FITC, CD62L-allophycocyanin, CD44-allophycocyanin/PE-Cy7, CD25-allophycocyanin, and Foxp3-PE were purchased from BD Biosciences (San Jose, CA) or eBioscience (San Diego, CA). PDCA-1-PE and B220-FITC were purchased from Miltenyi Biotec. Intracellular staining for Foxp3 was carried out using the Treg staining kit from eBioscience.

Adoptive transfer of BMDCs in an induced model of colitis

BMDCs were generated using GM-CSF and IL-4, and 3×10^6 CD11c⁺ cells were i.p. injected into B6 *Rag1*^{-/-} mice that had received naive CD4⁺CD45RB^{hi} T cells 2 wk earlier. Ten days posttransfer, mice were sacrificed, and colons were collected for histological analysis and explants cultures. Cytokine expression was determined by quantitative RT-PCR.

Microarray analysis

Splenic CD11c⁺ DCs were magnetically (CD11c isolation kit; Miltenyi Biotec) sorted from at least three control or DC-*Tgfb β 2* KO mice. For isolation of MLN DCs, single-cell suspensions of the LNs were stained with a mixture of Abs consisting of CD45-Percp, MHCII-FITC, CD11c-allophycocyanin, CD11b-eFluor-450, and CD103-PE (all from eBioscience). Samples were sorted in a BD FACSaria at the Cytometry Core facility at the Arizona Cancer Center. Cells were gated on CD45⁺MHCII⁺ population and further gated on the combined population of CD11c⁺CD11b⁺ and CD11c⁺CD11b⁻ cells. These cells were then sorted based on CD103 expression. Samples were pooled from four different mice, and RNA was isolated using an RNAqueous-Micro kit (Ambion, Life Technologies) to yield three samples per genotype. RNA integrity was evaluated with Agilent 2100 BioAnalyzer microfluidics-based platform (Agilent Technologies, Foster City, CA). RNA samples were subsequently processed to yield biotinylated cRNA for hybridization to Affymetrix Mouse Exon 1.0 ST arrays. The expression data were obtained in the form of .CEL files and imported into GeneSpring GX 10.0.2 (Agilent Technologies)

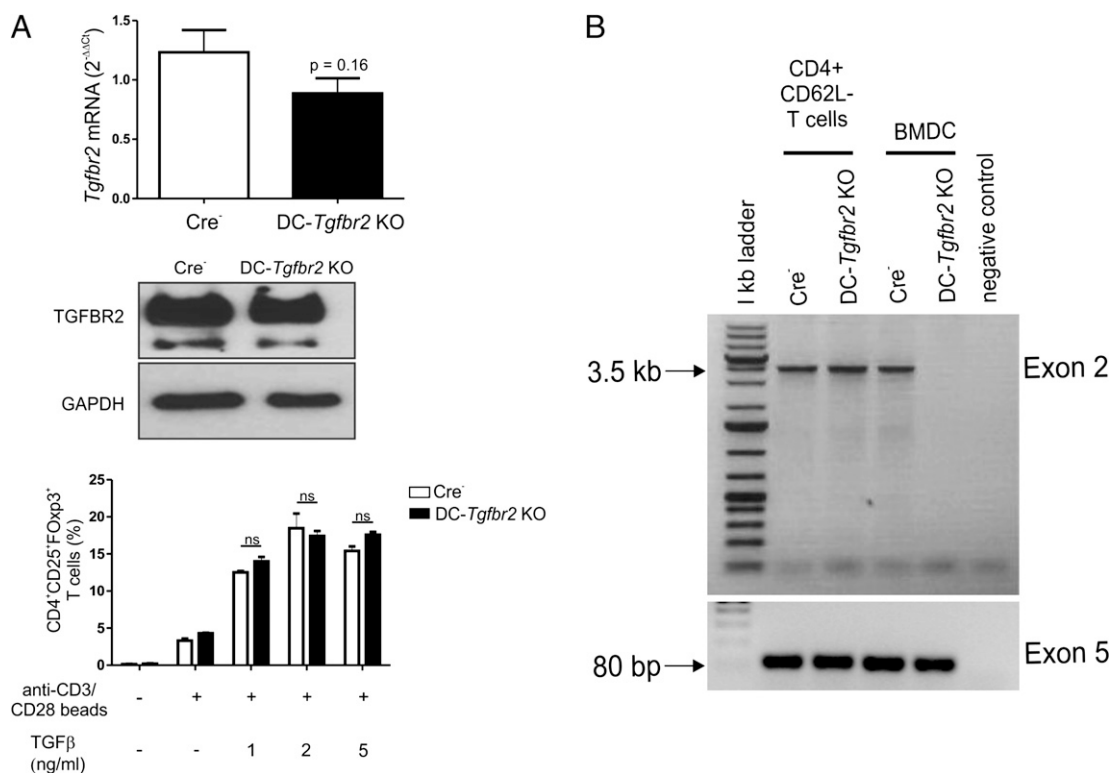


FIGURE 2. TGFBR2 expression in T cells. (A) *Tgfb2* mRNA expression in CD4⁺ T cells from the spleen of Cre⁻ and DC-*Tgfb2* KO mice (top panel). Each sample was normalized to TBP expression. Error bars represent means + SEM of five individual mice; TGFBR2 expression in CD4⁺CD62L⁺ T cells from the spleen of Cre⁻ and DC-*Tgfb2* KO mice (middle panel). GAPDH was used as a loading control. Data are representative of at least three different experiments; percentage of CD4⁺CD25⁺Foxp3⁺ T cells generated after stimulation of naive CD4⁺CD62L⁺ T cells with anti-CD3/CD28 beads and indicated concentrations of TGF- β for 3 d (bottom panel). Error bars represent means + SEM ($n = 3$). Student *t* test. (B) PCR detection of Cre-mediated excision of exon 2 of *Tgfb2* in genomic DNA extracted from CD4⁺CD62L⁺ T cells from control or DC-*Tgfb2* KO mice. CD11c⁺ BMDCs from either control or DC-*Tgfb2* KO mice were used as positive controls. Amplicon from exon 5 is shown as an input control.

software package for data quality control and statistical analysis of the microarray data. Stringent empirical and statistical analyses were used to compare gene expression profiles between Cre⁻ and DC-*Tgfb β 2* KO mice with cross-gene error model based on replicates (data deposited to Gene Expression Omnibus database [http://www.ncbi.nlm.nih.gov/geo/]; accession code GSE39651).

Western blot analysis

Whole-cell lysates were collected in radioimmunoprecipitation assay buffer, and protein concentration in lysates was determined using bicinchoninic acid reagent (Thermo Fisher Scientific, Rockford, IL). Twenty micrograms of protein was subjected to SDS-PAGE electrophoresis, and separated proteins were transferred on to nitrocellulose membrane (Bio-Rad Laboratories, Hercules, CA), blocked at least for 1 h in 5% BSA or milk in 1× TBS buffer containing 0.1% Tween 20 (TBST), and probed with pSmad2 (Cell Signaling Technology, Danvers, MA) or TGFBR2 (Santa Cruz Biotechnology, Santa Cruz, CA) Ab overnight at 4°C. The membranes were washed three times with TBST buffer, followed by incubation with appropriate HRP-coupled secondary Ab. Super Signal West Pico detection kit (Thermo Fisher Scientific, Rockford, IL) was used for

chemiluminescent detection. Blots were probed for total Smad2 or GAPDH to confirm equal loading.

Autoantibodies were detected according to a previously described protocol (24).

Real-time PCR

Total RNA was isolated from tissues or cells using TRIzol reagent (Life Technologies), and its integrity was confirmed by denaturing agarose gel electrophoresis and calculated densitometric 28S/18S ratio. Total RNA (250 ng) was reverse transcribed using iScript cDNA synthesis kit (Bio-Rad Laboratories). Subsequently, 20 μ l PCRs were set up in 96-well plates containing 10 μ l 2× IQ Supermix (Bio-Rad Laboratories), 1 μ l TaqMan respective primer/probe set (Applied Biosystems, Foster City, CA), 2 μ l of the cDNA synthesis reaction (10% of reverse transcription reaction), and 7 μ l nuclease-free water. Reactions were run and analyzed on a Bio-Rad CFX96 iCycler real-time PCR detection system. Cycling parameters were determined, and resulting data were analyzed by using the comparative threshold cycle (Ct) method as means of relative quantification, normalized to an endogenous reference (TATA box binding protein [TBP]) and relative to a calibrator (normalized Ct value obtained from control mice) and

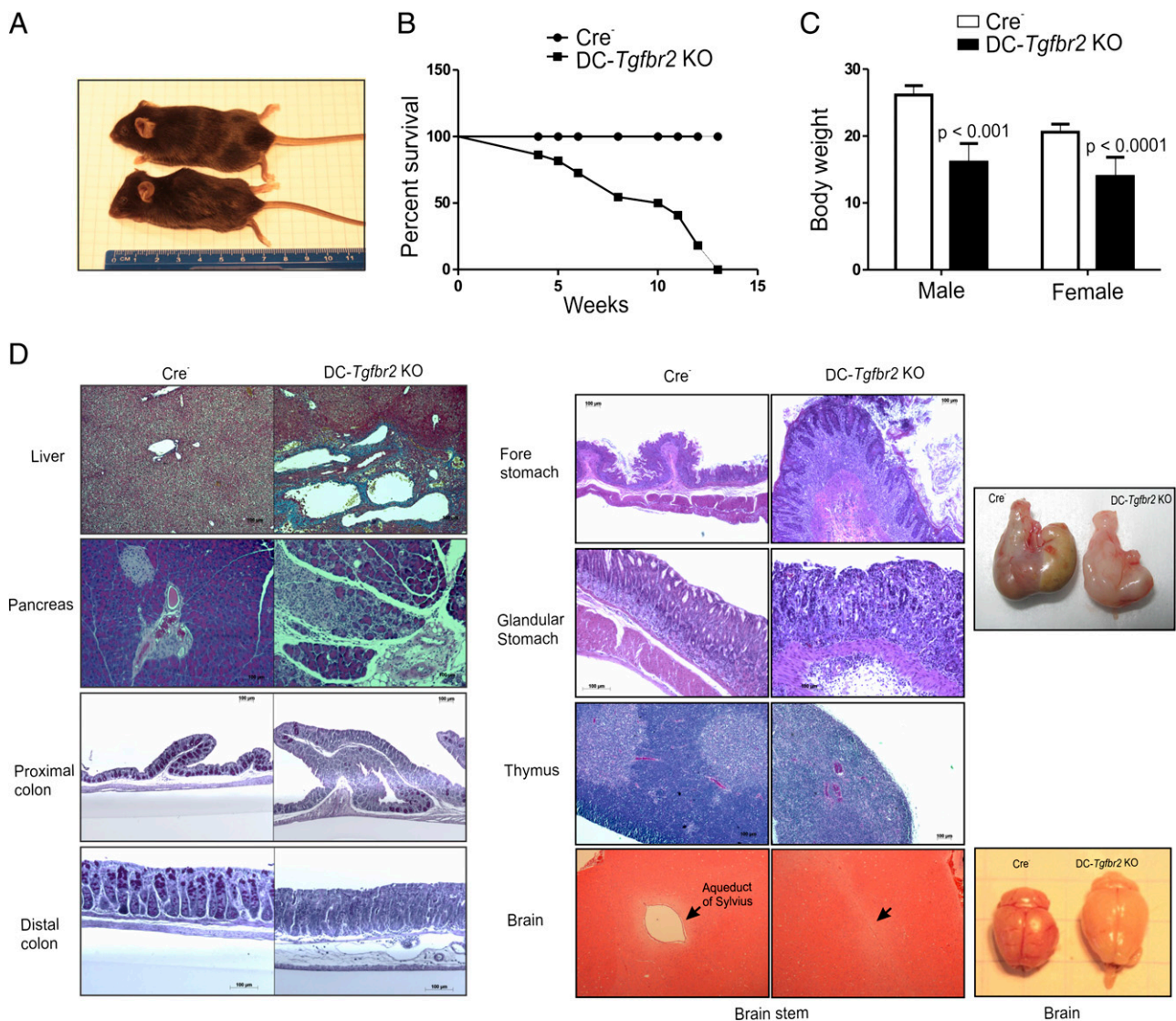


FIGURE 3. Pathology of DC-*Tgfb β 2* KO mice. (A) Photograph of a 12-wk-old DC-*Tgfb β 2* KO mouse along with its littermate control mouse demonstrating hydrocephalus, hunched back, and reduced body weight in DC-*Tgfb β 2* KO mouse. (B) Survival curve of DC-*Tgfb β 2* KO mice and controls ($n = 22$ for each, includes males and females); (C) body weight of Cre⁻ and DC-*Tgfb β 2* KO mice at 12 wk of age. Error bars represent means + SEM ($n = 4$ –6 males and 10–14 females). The p values were obtained using a Student t test. (D) Histology of indicated tissue sections from 12-wk-old Cre⁻ and DC-*Tgfb β 2* KO mice (representative results of ≥ 5 mice; original magnification $\times 100$). Sections of the liver were stained with Trichrome staining and those of the colon were stained with periodic acid-Schiff staining. Histology images labeled as “Brain stem” (original magnification $\times 20$). Other tissue sections were stained with H&E. Gross morphology of the stomach and brain from Cre⁻ (left) and DC-*Tgfb β 2* KO (right) mice are shown on the far right.

expressed as $2^{-\Delta\Delta C_t}$ (Applied Biosystems User Bulletin number 2: Rev B "Relative Quantification of Gene Expression").

Histology

Tissues were fixed in 10% formalin and embedded in paraffin, and 5- μ m sections were stained with H&E.

Immunohistochemistry

Sections of the liver, stomach, and pancreas were harvested, fixed in Tissue-Tek (Sakura Finetek, Torrance, CA), and snap frozen in liquid nitrogen. Sections (5 μ m) were cut, mounted on slides, and fixed for 10 min in cold methanol. After washing in $1\times$ TBS, residual endogenous peroxidase activity was quenched by incubation in 3% H_2O_2 in water for 10 min. Slides were then incubated with 5% normal goat serum (Vector Laboratories, Burlingame, CA) for 1 h in TBST. Next, sections were incubated with a primary Ab against CD4 differentiation Ag (1/50; BD Biosciences) in TBST overnight at 4°C. After three washes in TBST, slides were incubated with biotinylated secondary Ab and avidin/peroxidase complex according to the manufacturer's recommendation (Vector Laboratories). Slides were then incubated with 3,3'-diaminobenzidine (Vector Laboratories) and mounted with Dako mounting medium (Dako North America, Carpinteria, CA). Slide examination was performed independently by two experienced scientists in a blind manner using a Zeiss Axioplan microscope (Carl Zeiss MicroImaging, Thornwood, NY). Images were captured with Nikon Digital Sight DS-Fi1 camera and NIS-Elements Imaging Software (Nikon Instruments, Melville, NY).

ELISA and multiplex assays

Cytokines in cell culture supernatants or colonic explant cultures were detected using appropriate ELISA kits from eBioscience. Igs in serum were detected using Mouse Ig isotyping kit (EMD Millipore, Billerica, MA) on a Luminex-100 workstation (Liquichip; Qiagen) and analyzed using MasterPlex 2010 software (Hitachi Solutions America, MiraiBio Group, South San Francisco, CA).

Treg conversion assay

CD11c⁺ Flt3L BMDCs were pretreated with indicated concentrations of OVA (Sigma-Aldrich, St. Louis, MO) for 18 h, washed three times with CM, and cocultured with CD4⁺CD62L⁺ T cells from the spleens of OT-II

mice in the presence or absence of 5 ng/ml TGF- β . Cells were incubated for 90 h at 37°C. CD11c⁺ MLN DCs were cocultured with naive OT-II T cells in the presence of 1 mg/ml OVA and 5 ng/ml TGF- β for 90 h at 37°C. Foxp3 staining was performed as described earlier. In some conditions, an anti-IFN- γ neutralizing Ab (2 μ g/ml, clone XMG 1.2; eBioscience) or an isotype control Ab (rat IgG1) was used.

iTreg generation

CD4⁺CD62L⁺ T cells from wild-type mice were stimulated with anti-CD3/anti-CD28 beads (Life Technologies), TGF- β (5 ng/ml), IL-2 (20 ng/ml; PeproTech), and 0.5 μ M retinoic acid (Sigma-Aldrich) for 4 d. More than 85% of T cells expressed Foxp3 on day 4 as determined by flow cytometry (data not shown).

Statistical analysis

Statistical analyses were performed using GraphPad Prism software (GraphPad Software, La Jolla, CA) using one-way ANOVA, followed by a Newman-Keuls or Bonferroni post hoc test or by a Student *t* test, whenever appropriate.

Results

Specificity of *Tgfb2* deletion in DC-*Tgfb2* KO mice

Initial comparison of wild-type and *Cre⁻/Tgfb2^{fl/fl}* (B6.129S6-*Tgfb2^{tm1Hhm}*) mice revealed no effect of loxP sites on TGFBR2 protein or mRNA expression (data not shown). Therefore, *Cre⁻/Tgfb2^{fl/fl}* mice (referred to as *Cre⁻*) were used as control mice throughout the study. Efficient reduction of *Tgfb2* mRNA was confirmed by quantitative PCR (qPCR) in CD11c⁺ BMDCs from DC-*Tgfb2* KO mice (Fig. 1A). Phosphorylation of Smad2 induced by exogenous TGF- β was also significantly reduced in BMDCs (Fig. 1B) from DC-*Tgfb2* KO mice compared with BMDCs from control *Cre⁻* littermates. In splenic DCs from DC-*Tgfb2* KO mice, TGFBR2 protein expression was significantly reduced compared with those from *Cre⁻* mice (Fig. 1C). However, TGFBR2 protein expression was not affected in other CD11c^{lo} cell types including B cells, NK cells, and macrophages from DC-*Tgfb2* KO mice (Fig. 1D-F). *Tgfb2* mRNA was decreased by

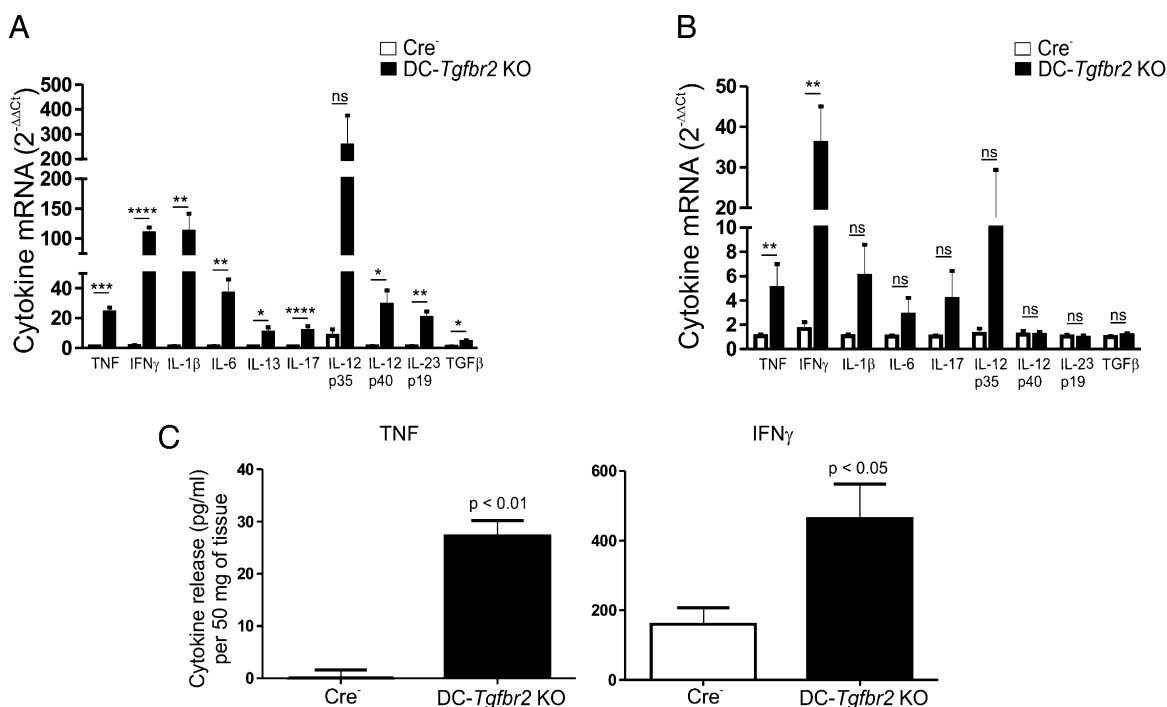


FIGURE 4. Elevated cytokine expression in DC-*Tgfb2* KO mice. (A and B) mRNA expression of indicated cytokines in the forestomach (A) and proximal colon (B) of *Cre⁻* and DC-*Tgfb2* KO mice. Samples were normalized to TBP. Error bars represent means + SEM of samples from five mice. **p* < 0.05, ***p* < 0.01, ****p* < 0.001, *****p* < 0.0001 (Student *t* test). (C) TNF and IFN- γ expression in the colonic explant cultures of *Cre⁻* and DC-*Tgfb2* KO mice. Results are expressed as cytokine release per 50 mg of tissue. Error bars represent means + SEM of at least six individual mice. All *p* values were obtained using a Student *t* test.

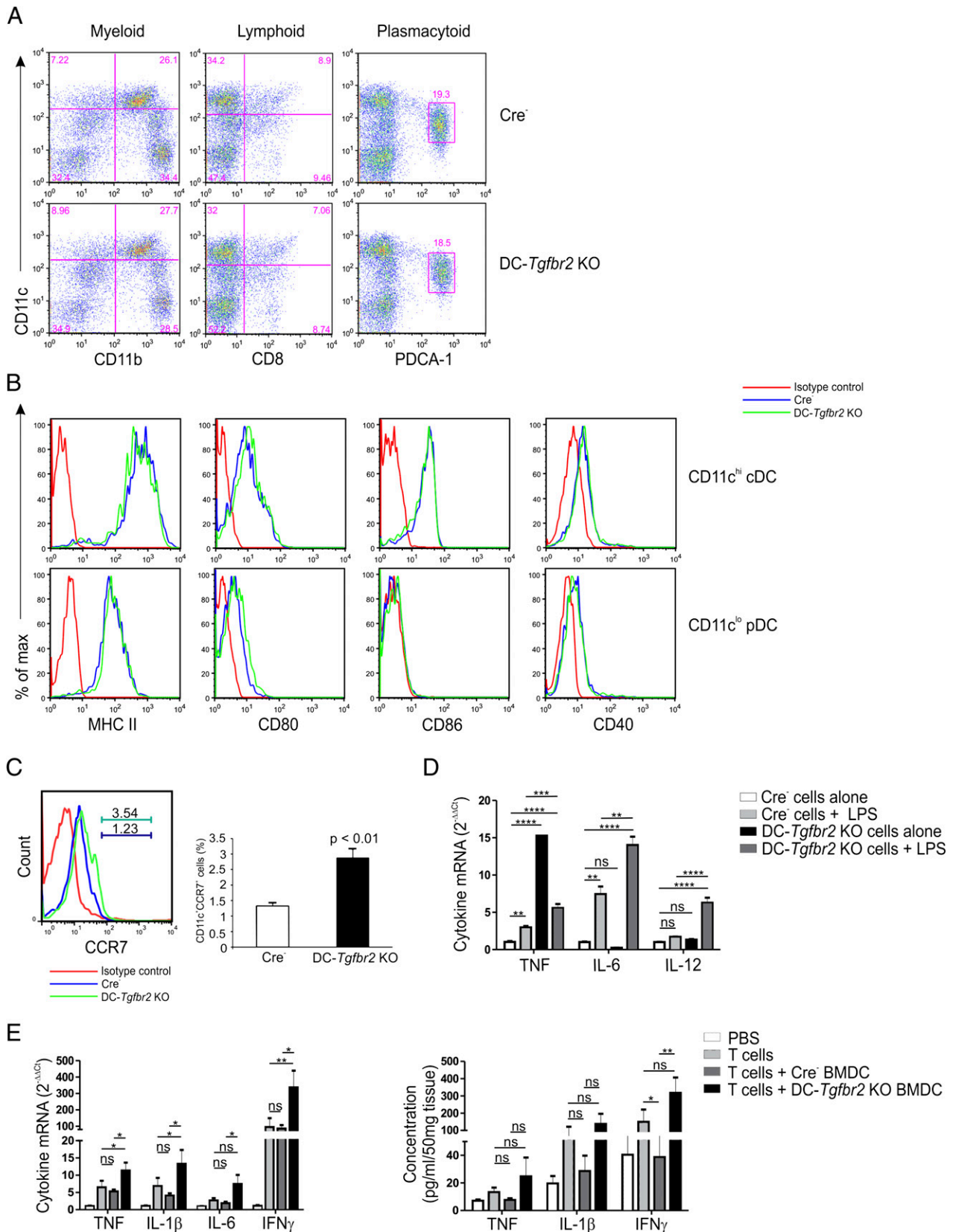


FIGURE 5. *Tgfb2* KO DCs are more proinflammatory. (**A**) Staining of indicated DC subsets in the CD19- and DX5-depleted splenocytes from 8-wk-old Cre^{-/-} (top panel) and DC-*Tgfb2* KO (bottom panel) mice. Dot plots are gated on CD3⁻ cells (data representative of at least four different experiments); (**B**) MHCII, CD80, CD86, and CD40 on CD11c^{hi} splenic classical DCs (cDCs) (top panel) and CD11c^{lo}PDCA-1⁺ pDCs (bottom panel) of Cre^{-/-} and DC-*Tgfb2* KO mice. Cells were prepared and gated as described in (A). Data representative of at least four experiments; (**C**) CCR7 expression in CD11c⁺ splenic DCs from Cre^{-/-} and DC-*Tgfb2* KO mice. Bar graph represents the frequency of CD11c⁺CCR7⁺ DCs in the spleen of Cre^{-/-} and DC-*Tgfb2* KO mice are indicated on the right. Error bars represent means + SEM of ≥ 6 mice. All p values obtained using a Student t test. (**D**) Cytokine mRNA expression in CD11c⁺ BMDCs differentiated with GM-CSF and IL-4 \pm LPS for 18 h. Samples were normalized to TBP. Error bars represent (Figure legend continues)

28% in total splenic CD4⁺ T cells isolated from DC-*Tgfb2* KO mice, although without reaching statistical significance ($p > 0.16$) (Fig. 2A, *top panel*). There was no difference in TGFBR2 protein expression in naive splenic CD4⁺CD62L^{hi} T cells (Fig. 2A, *middle panel*). Moreover, we demonstrated the same rates of iTreg (CD25⁺Foxp3⁺) conversion from naive CD4⁺CD62L⁺ T cells isolated from the spleen of Cre⁻ or DC-*Tgfb2* KO mice in the presence of TGF- β and anti-CD3/anti-CD28 beads, thus confirming intact TGF- β signaling in naive T cells (Fig. 2A, *bottom panel*). We have also adoptively transferred naive CD4⁺CD45Rb^{hi} T cells from Cre⁻ or DC-*Tgfb2* KO mice into Rag1^{-/-} recipients and observed no difference in the pathogenic (colitis) effects of the T cells from the two donor strains (data not shown). To address potential Cre-mediated recombination in activated CD4⁺CD11c^{lo} T cells, we isolated genomic DNA from splenic CD4⁺CD62L⁻ T cells from healthy Cre⁻ and symptomatic DC-*Tgfb2* KO mice and performed PCR with primers specific to exon 2 (and exon 5 as input control) of *Tgfb2* gene. Efficient recombination of exon 2 could only be demonstrated in CD11c⁺ BMDCs but not in activated T cells from DC-*Tgfb2* KO mice (Fig. 2B). Collectively, these data demonstrate efficient deletion of *Tgfb2* and abrogation of TGF- β signaling specifically in DCs.

Absence of TGF- β signaling in DCs leads to multiorgan autoimmune inflammation

DC-*Tgfb2* KO mice were phenotypically normal until ~3–4 wk of age; they became symptomatic and moribund by 4–14 wk of age (Fig. 3A, 3B) and gradually developed wasting disease with body weight reduced by ~30–40% in surviving mice at 12 wk of age (Fig. 3C). Histopathology of DC-*Tgfb2* KO mice revealed mild-to-moderate subacute multifocal hepatitis with focal fibrosis (Fig. 3D); mild-to-severe subacute multifocal pancreatitis with loss of exocrine cells (Fig. 3D); mild-to-moderate subacute multifocal colitis with loss of goblet cells; and mild-to-moderate crypt hyperplasia and predominantly lymphocytic or mixed lymphocytic and neutrophilic infiltrates (Fig. 3D) and severe subacute diffuse gastritis with mucosal hyperplasia (Fig. 3D). Premature involution of the thymus with complete loss of the thymic cortex was also observed in DC-*Tgfb2* KO mice. DC-*Tgfb2* KO mice also developed hydrocephalus, which was confirmed histologically to be because of the complete blockage of Aqueduct of Sylvius and dilation of lateral ventricles (Fig. 3D). DC-*Tgfb2* KO mice had elevated proinflammatory cytokine expression both in the stomach and in the colon (Fig. 4A, 4B). In addition, TNF and IFN- γ secretion was significantly elevated in colonic explant cultures from DC-*Tgfb2* KO mice (Fig. 4C). These findings reveal that loss of TGF- β signaling in DCs leads to widespread autoimmune inflammation in multiple organs of the digestive tract. Similar mortality and pathology has been observed in DC-*Tgfb2* KO rederived via embryo transfer into an ultraclean *Helicobacter sp.*-negative environment (data not shown).

Tgfb2 deficiency does not affect differentiation of major DC subtypes or MHCII and costimulatory molecule expression in vivo

To determine whether lack of TGF- β signaling in DCs affects their differentiation, we looked at the major DC subsets in the spleen and LNs of DC-*Tgfb2* KO mice using flow cytometry. Splenocytes depleted of B and NK cells or MLN cells were stained with

a mixture of Abs to identify the myeloid (CD11c^{hi}CD11b⁺), lymphoid (CD11c^{hi}CD8⁺), and plasmacytoid (CD11c^{lo}PDCA-1⁺) population of DCs, based on the gating strategy described in Supplemental Fig. 1. We found no significant difference in the frequency of different subsets between Cre⁻ and Cre⁺ mice both in the spleen and MLN (Fig. 5A; data not shown). Contrary to in vitro observations (3), there was no difference in the expression of MHCII, CD80, CD86, or CD40 in either CD11c^{hi} classical DCs or plasmacytoid DCs (pDCs) in the spleen and MLN of DC-*Tgfb2* KO at 10 wk of age (Fig. 5B; data not shown). However, we observed a significant increase in the frequency of CD11c⁺CCR7⁺ DCs in the spleen and MLN of DC-*Tgfb2* KO mice (Fig. 5C; data not shown) indicating increased presence of migratory DCs. Therefore, on the basis of MHCII and costimulatory molecule expression, loss of TGF- β signaling in DCs is unlikely to affect their Ag-presenting capacity in vivo.

DC from DC-*Tgfb2* KO mice are more proinflammatory

TGF- β prevents the development of a subset of inflammatory DCs that express E-cadherin (6). Consistently, we observed a similar increase in the frequency of E-cadherin⁺CD11c⁺ DCs in the MLN of DC-*Tgfb2* KO mice (Supplemental Fig. 2), thus suggesting that *Tgfb2*-deficient DCs are indeed more proinflammatory. To test this hypothesis, we analyzed major proinflammatory gene expression by qPCR in CD11c⁺ BMDCs generated from 4- to 6-wk-old asymptomatic mice. DCs from DC-*Tgfb2* KO mice had significantly elevated expression of TNF, even at the basal level as compared with control mice. LPS treatment did not further increase TNF expression, but IL-6 and IL-12 were significantly upregulated compared with Cre⁻ DCs (Fig. 5D). To functionally test the proinflammatory potential of *Tgfb2* KO DCs, we examined their ability to affect the early stages of T cell-mediated colitis. Rag1^{-/-} mice received CD4⁺CD45RB^{hi} T cells 2 wk prior to adoptive transfer of CD11c⁺ BMDCs and were monitored for another 10 d, after which time, the degree of colonic inflammation was assessed based on the proinflammatory gene expression profile. Administration of *Tgfb2* KO DCs but not Cre⁻ DCs led to a significant increase in the colonic gene expression of TNF, IL-1 β , IL-6, and IFN- γ (Fig. 5E, *left panel*). Although with the exception of IFN- γ , cytokine secretion from colonic explants did not reach significance (likely because of the early stage of colitis selected because of short lifespan of transferred DCs), they were markedly elevated compared with mice injected with Cre⁻ DCs (Fig. 5E, *right panel*). These results demonstrate that *Tgfb2* KO DCs are more proinflammatory and can exacerbate T cell-mediated pathology.

We also performed a complete gene expression profiling in total splenic CD11c⁺ DC population and MLN CD11c⁺CD103⁺ DCs isolated from 8-wk-old Cre⁻ or asymptomatic DC-*Tgfb2* KO mice using mouse Exon ST1.0 arrays (Affymetrix). Two hundred seventy-eight and 208 genes were differentially regulated in splenic DCs and MLN DCs, respectively, from DC-*Tgfb2* KO mice (up- or down-regulated; $p < 0.05$) with a fold change of ≥ 1.3 (Fig. 6A, 6D). These genes were categorized based on their biological function and sorted according to the Expression Analysis Systematic Explorer score (Fig. 6B, 6E). Among the genes involved in Th1 type inflammatory responses, we found upregulation of *TNF* (1.7-fold) in splenic DCs and *IFN γ* (~2-fold) in MLN DCs. In addition, we found increased

means \pm SEM of triplicate samples; (E) relative mRNA (*left panel*) and protein (*right panel*) expression of indicated cytokines in the colon of Rag1^{-/-} mice transferred with or without CD4⁺CD45RB^{hi} naive T cells (0.5×10^6 cells), followed by either Cre⁻ or DC-*Tgfb2* KO BMDCs (3×10^6 cells). Samples were normalized to TBP. Error bars represent SEM of at least five to six mice per group. Protein expression in colonic explant cultures was determined by ELISA. * $p < 0.05$, ** $p < 0.01$, *** $p < 0.001$, **** $p < 0.0001$ (one-way ANOVA with a Bonferroni post hoc test).

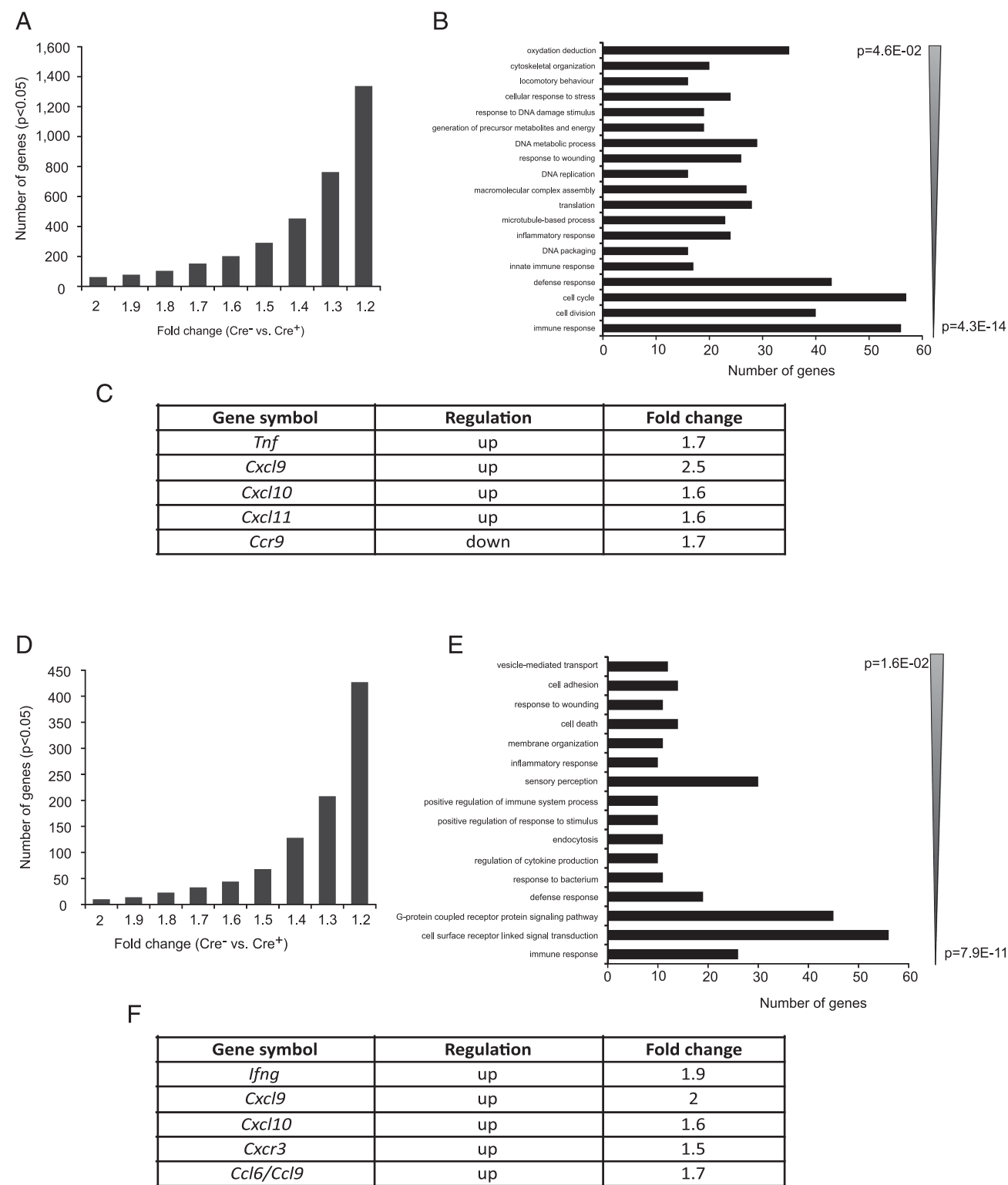


FIGURE 6. Microarray analysis of *Tgfb β 2* KO DCs. **(A)** Histogram depicting the number of genes/probe sets whose expression was increased or reduced at $p < 0.05$ in CD11c $^+$ splenic DCs from DC-*Tgfb β 2* KO mice relative to their wild-type littermates. Increasing stringency of analysis (1.2- to 2-fold change on x-axis) demonstrates the magnitude of change in splenic DC gene expression profile in DC-*Tgfb β 2* KO mice; **(B)** gene ontology analysis using the Database for Annotation, Visualization and Integrated Discovery functional annotation tool (<http://david.abcc.ncifcrf.gov/>) of the 535 gene/probe sets, which indicated >1.4 -fold change at $p < 0.05$ (Student t test with Benjamini and Hochberg false-discovery rate as multiple testing correction). Genes categorized based on biological process were grouped and ranked (threshold of 5; $p < 0.05$). Categories were sorted according to the Expression Analysis Systematic Explorer score, a modified Fisher exact p value; **(C)** table of genes up- or downregulated in DC-*Tgfb β 2* KO mice as compared with Cre^- mice; **(D, E)** same as described in **(A)** and **(B)** but depicts the gene expression changes in MLN CD11c $^+$ CD103 $^+$ DCs from DC-*Tgfb β 2* KO mice as compared with Cre^- mice; **(F)** selected genes upregulated in DC-*Tgfb β 2* KO mice as compared with Cre^- mice. $n = 3/\text{genotype}$ with RNA pooled from at least four mice per sample.

mRNA expression of the T cell chemoattractants *CXCL9*, *CXCL10*, *CXCL11*, *CCL6*, and *CCL9* (Fig. 6C, 6F). Expression of *CCR9* chemokine receptor, which may be used to discriminate between immature and mature DCs (25), was downregulated (Fig. 6C), thus suggesting a more mature phenotype of *Tgfb2* KO DCs. The results of the microarray analysis confirm that *Tgfb2*-deficient DCs are more proinflammatory and the observed pathology in DC-*Tgfb2* KO mice may be at least in part because of increased production of proinflammatory cytokines like TNF and IFN- γ , which augment Th1 inflammatory responses.

TGF- β has been shown to induce IDO expression in DC through autocrine signaling (9). However, our microarray results did not reveal lower expression of IDO both in splenic as well as MLN DCs from DC-*Tgfb2* KO mice. To confirm these results, we determined IDO expression in splenic CD11c⁺ DCs by Western blot analysis and real-time PCR, respectively. As shown in Fig. 7A and 7C, we did not find any significant difference in the baseline IDO expression at the protein or transcript in splenic DCs between Cre⁻ and Cre⁺ mice. Similarly, we observed the same pattern of IDO mRNA expression in MLN CD11c⁺ DC (Fig. 7B). In addition, we also treated both splenic and BM-derived CD11c⁺ DCs with IFN- γ or TGF- β 1 and analyzed IDO expression. Consistently, we detected no difference in the basal expression of IDO between Cre⁻ and Cre⁺ mice and no significant effect of TGF- β 1-stimulated IDO expression in DCs from Cre⁺ mice. The response to IFN- γ was largely preserved in both strains, albeit somewhat dampened by TGFBR2 deficiency (Fig. 7C, 7D).

Impaired TGF- β signaling in DCs leads to T and B cell activation

As previously described, DC-*Tgfb2* KO mice display premature thymic involution and thymocytes from 10-wk-old DC-*Tgfb2* KO

mice showed a 2-fold increase in the frequency of CD4 single-positive (SP) cells, although the total numbers were not significantly different from Cre⁻ mice (Fig. 8A). However, there was a significant increase in both the frequency and number of Qa2⁺ CD24^{lo} cells among the CD4 SP population in DC-*Tgfb2* KO mice compared with Cre⁻ mice, suggesting that the increased frequency of CD4⁺ SP cells was a result of recirculation of peripheral CD4 T cells into the thymus, a classic phenomenon in autoimmunity (Fig. 8B) (26). We found a marked increase in the frequency of CD62L^{lo}CD44^{hi} cells among both CD4⁺ and CD8⁺ T cells in the periphery (spleen and MLN) of DC-*Tgfb2* KO mice (Fig. 8C, Supplemental 3A, 3B). Consistent with these findings, we also demonstrated CD4⁺ T cell infiltration by immunohistochemistry in the stomach, pancreas, and liver of DC-*Tgfb2* KO mice but not in Cre⁻ mice (Supplemental Fig. 3C).

DC-*Tgfb2* KO mice had significantly increased levels of serum IgG1 and IgM (Fig. 9A). To test for the presence of autoantibodies, we probed tissue lysates from *Rag*^{-/-} mice with serum from either Cre⁻ or DC-*Tgfb2* KO mice. Several distinct bands were observed only in tissues probed with serum from DC-*Tgfb2* KO mice (Fig. 9B). Overall, these results suggest that abrogation of TGF- β signaling in DCs result in spontaneous activation of self-reactive T and B cells.

Alteration of Treg phenotype in DC-*Tgfb2* KO mice

Loss of CD4⁺CD25⁺Foxp3⁺ Tregs leads to a fatal multiorgan autoimmune syndrome (27). To determine whether a similar loss of Tregs in DC-*Tgfb2* KO mice was responsible for the autoimmune pathology, we looked at Treg frequency and numbers in the lymphoid organs of DC-*Tgfb2* KO mice. In 4-wk-old mice with intact thymus, we found no significant difference in the percentage of thymic CD4⁺Foxp3⁺ T cells between Cre⁻ and DC-*Tgfb2* KO

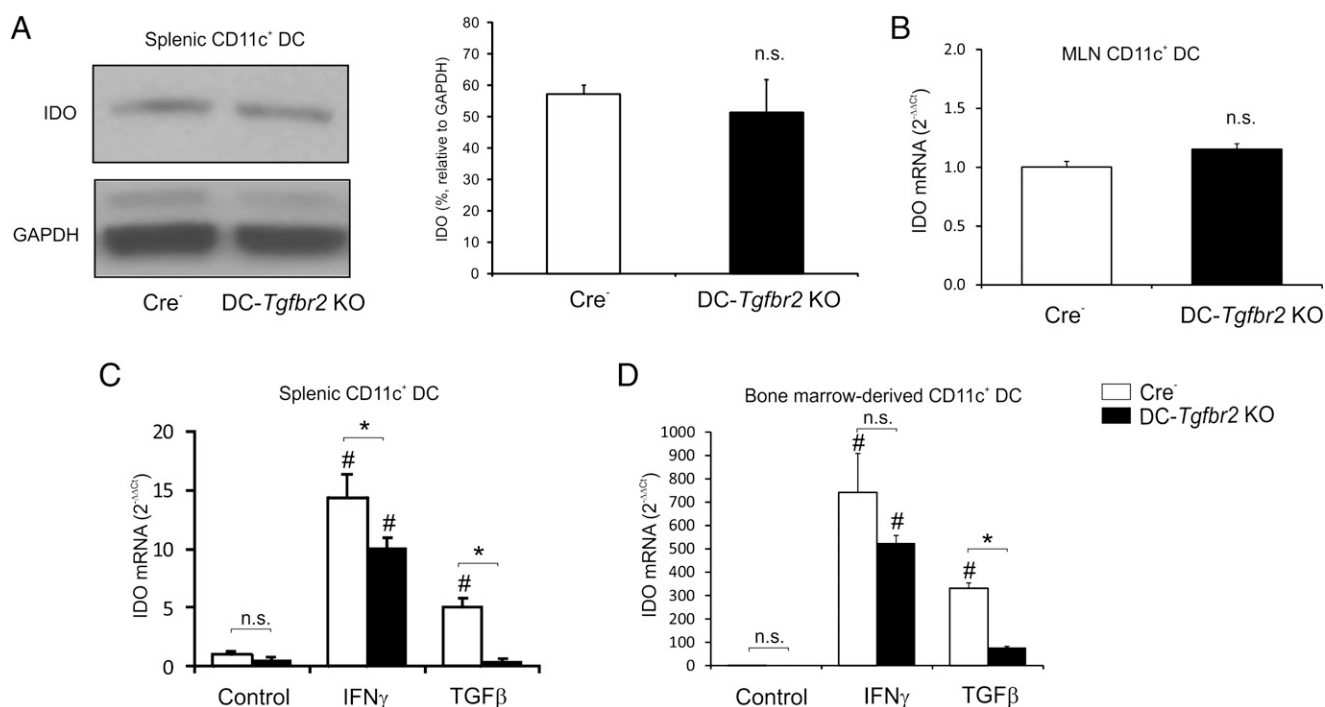


FIGURE 7. Lack of TGF- β signaling in DCs does not affect IDO expression. (A) Western blot analysis for IDO expression in splenic CD11c⁺ DCs from control and DC-*Tgfb2* KO mice. Corresponding densitometric analysis of the Western blot relative to GAPDH is shown on the right. Error bars represent means + SEM of three individual mice. (B) IDO mRNA expression in MLN CD11c⁺ DCs. Each sample was normalized to TBP expression. Error bars represent means + SEM of three individual mice. (C and D) mRNA expression of IDO in splenic (C) or BM-derived CD11c⁺ DCs (D) treated with or without IFN- γ (200 U/ml) or TGF- β (20 ng/ml) for 18 h. Each sample was normalized to TBP expression. Error bars represent means + SEM of three repetitions. The *p* values were obtained using one-way ANOVA, followed by a Newman-Keuls post hoc test. **p* < 0.05 in Cre⁻ versus DC-*Tgfb2* KO within respective treatment, #*p* < 0.05 control versus IFN- γ or control versus TGF- β within respective genotype.

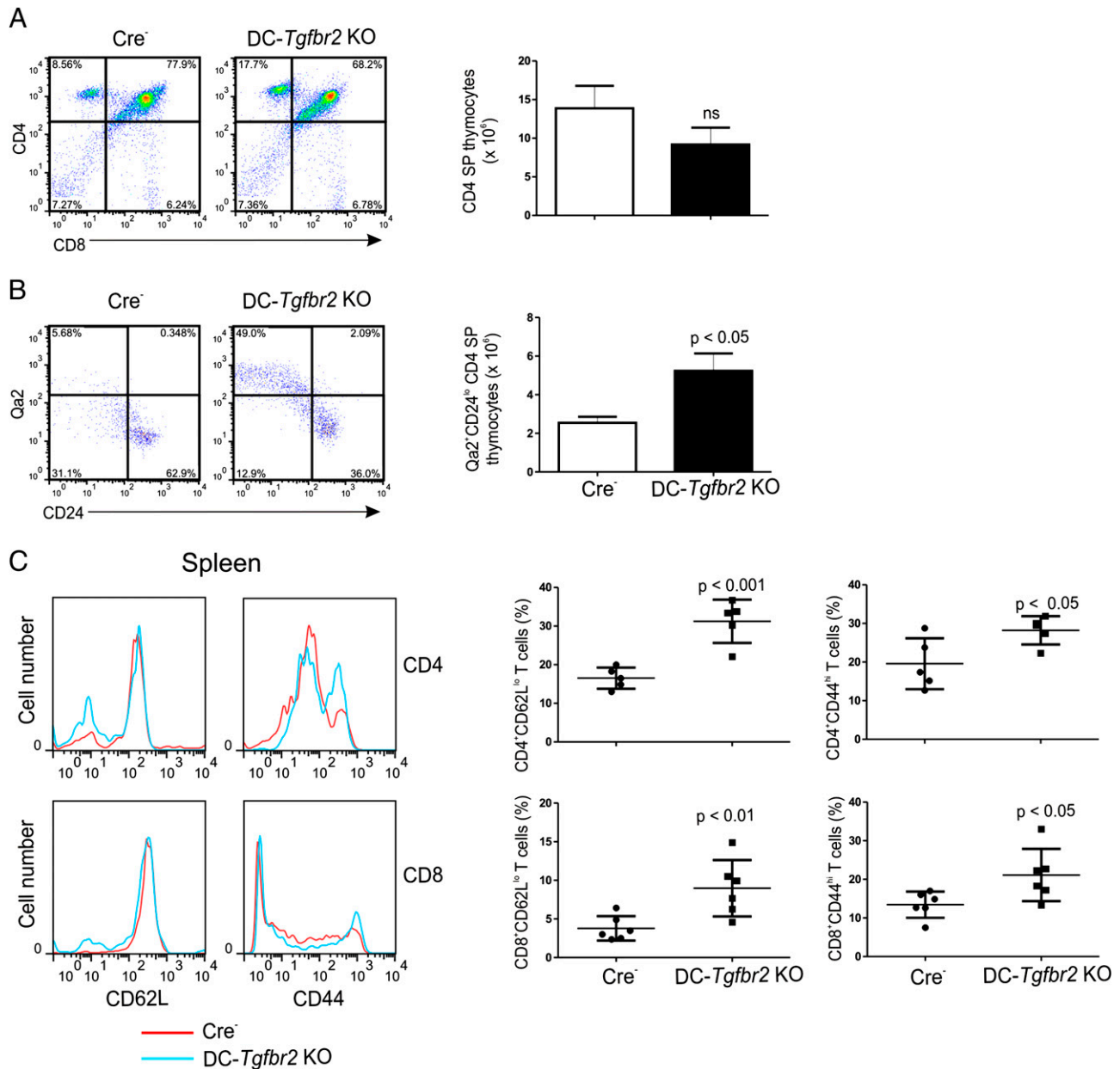


FIGURE 8. Deficient TGF- β signaling in DCs results in T cell activation. **(A)** CD4⁺ and CD8⁺ thymocytes in 10-wk-old Cre⁻ and DC-*Tgfr2* KO mice. The numbers of CD4⁺ SP cells are indicated on the right (representative of ≥ 6 mice). Bars represent means \pm SEM; **(B)** Qa2⁺ and CD24⁺ thymocytes in mice as described in **(A)** (gated on CD4⁺ SP cells). The numbers of Qa2⁺CD24^{lo}CD4 SP cells are indicated on the right (representative of ≥ 6 mice). Error bars represent means \pm SEM of ≥ 6 mice; **(C)** CD62L (left panels) and CD44 (right panels) expression among CD4⁺ (top panel) and CD8⁺ (bottom panel) splenic T cells from Cre⁻ and DC-*Tgfr2* KO mice. Percentage of CD62L^{lo} and CD44^{hi} CD4 (top panel) and CD8 (bottom panel) splenic T cells of control Cre⁻ and DC-*Tgfr2* KO mice are shown on the right. Bars represent means \pm SEM from five to six mice. All *p* values were obtained using a Student *t* test.

mice (Fig. 10A, left panel). With involution of the thymus at 10 wk, the frequency of CD4⁺Foxp3⁺ T cells increased in DC-*Tgfr2* KO mice, but the total numbers were not significantly different (Fig. 10A, middle and right panels). Interestingly, the proportion (both percentage and number) of CD4⁺Foxp3⁺ T cells in the spleen and MLN was increased in DC-*Tgfr2* KO mice compared with Cre⁻ mice (Fig. 10B), but the intensity of Foxp3 expression was significantly reduced in CD4⁺ T cells from DC-*Tgfr2* KO mice (Fig. 10C). Although in Cre⁻ mice almost all Foxp3⁺ cells were CD25⁺ (Fig. 11), in DC-*Tgfr2* KO mice, there was a considerable decrease in the proportion of CD25⁺Foxp3⁺ cells and an expansion of CD25⁻Foxp3⁺ cell population (Fig. 11A–C). These results suggest that the phenotype of peripheral Tregs in DC-*Tgfr2* KO mice is altered, which in turn may affect the function

of these cells (see Discussion), leading to or contributing to the development of autoimmunity.

Increased IFN- γ production by *Tgfr2* KO DCs inhibits Ag-specific Treg differentiation

In the presence of TGF- β , activation of naive T cells by DCs leads to the induction of Foxp3 transcription factor and Treg differentiation (19, 28). To determine whether DC-*Tgfr2* KO DCs are capable of driving Ag-specific Treg differentiation, we cocultured OVA-pretreated Flt3L-BMDCs from Cre⁻ or DC-*Tgfr2* KO mice with CD4⁺CD62L⁺ naive T cells from OT-II mice in the presence of recombinant TGF- β . Despite the presence of TGF- β , DCs from DC-*Tgfr2* KO mice were significantly less efficient in inducing CD4⁺CD25⁺Foxp3⁺ Treg differentiation than Cre⁻ DCs (Fig.

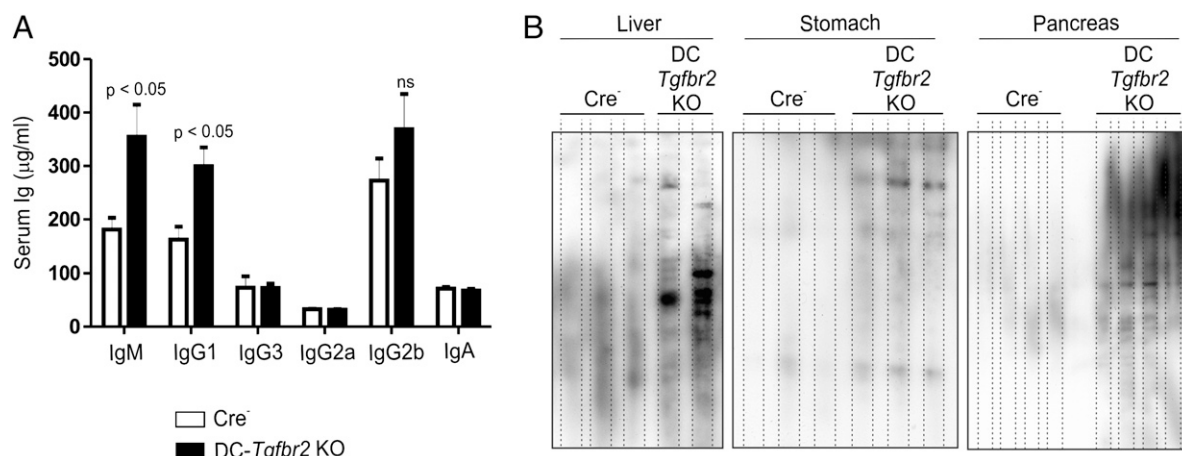


FIGURE 9. Deficient TGF- β signaling in DCs results in B cell activation. **(A)** Ig isotype concentrations in the serum of Cre⁻ and DC-*Tgfb2* KO mice. Error bars represent means + SEM of 10–12 mice/genotype; **(B)** Western blot analysis of indicated *Rag*^{-/-} tissue lysates showing the staining pattern of autoantibodies present in the serum of control ($n = 3$ –4) and DC-*Tgfb2* KO mice ($n = 2$ –4). All p values were obtained using a Student t test.

12A). We saw a similar effect at two different concentrations of OVA (data not shown). Analysis of cell coculture supernatants by ELISA revealed substantial increase in IFN- γ but not IL-6 levels

in DCs from DC-*Tgfb2* KO mice (Fig. 12B). qPCR analysis revealed ~40-fold increase in IFN- γ expression by Flt3L-BMDCs from DC-*Tgfb2* KO mice (Fig. 12C). To test whether IFN- γ

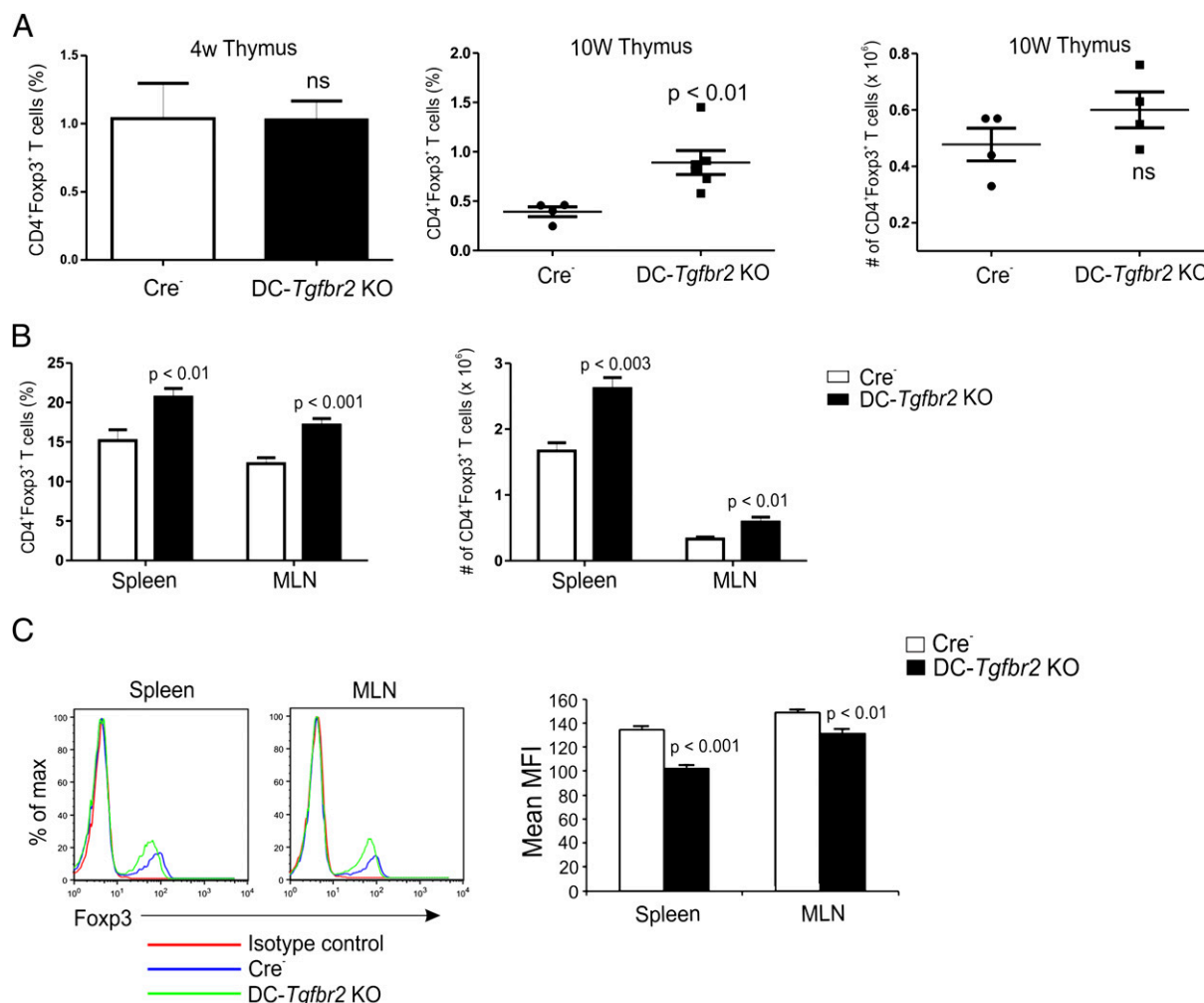


FIGURE 10. Altered Treg phenotype in DC-*Tgfb2* KO mice. **(A)** Left panel, Percentage of CD4⁺Foxp3⁺ T cells in the thymus of 4-wk-old DC-*Tgfb2* KO mice. Error bars represent means + SEM from at least three individual mice. Percentage (middle panel) and numbers (right panel) of CD4⁺Foxp3⁺ Tregs in the thymus of 10-wk-old control and DC-*Tgfb2* KO mice. Error bars represent means + SEM of six mice; not significant (ns), Student t test; **(B)** percentage (left panel) and numbers (right panel) of CD4⁺Foxp3⁺ Tregs in the spleen and MLN of 10-wk-old control and DC-*Tgfb2* KO mice. Error bars represent means + SEM of six mice; **(C)** Foxp3 expression in CD4⁺ T cells from the spleen and MLN of Cre⁻ and DC-*Tgfb2* KO mice (representative of ≥ 6 mice per group). Bar graph represents the mean fluorescence intensity of Foxp3 among CD4⁺ T cells in spleen and MLN of Cre⁻ and DC-*Tgfb2* KO mice. Error bars represent means + SEM of ≥ 6 mice.

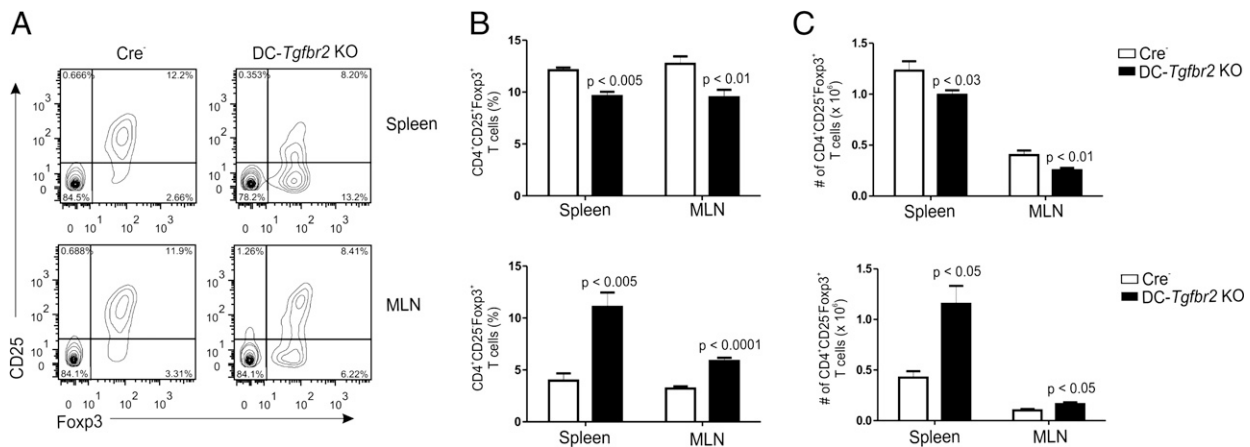


FIGURE 11. Expansion of CD25⁺Foxp3⁺ T cells in DC-Tgfb2 KO mice. **(A)** Contour plots showing the frequency of CD25⁺Foxp3⁺ (upper right quadrant) and CD25⁻Foxp3⁺ T cells (lower right quadrant) in the spleen (top panel) and MLN (bottom panel) of 8-wk-old asymptomatic control (left panel) and DC-Tgfb2 KO mice (right panel). Plots are gated on CD4⁺ cells; **(B)** percentage of CD4⁺CD25⁺Foxp3⁺ (top panel) and CD4⁺CD25⁻Foxp3⁺ (bottom panel) T cells in the spleen and MLN of control and DC-Tgfb2 KO mice. Error bars represent means + SEM of six mice. The *p* values were obtained using a Student *t* test; **(C)** bar graphs representing the number of CD25⁺ (top panel) and CD25⁻ (bottom panel) Foxp3⁺ T cells in the spleen and MLN of Cre⁻ and DC-Tgfb2 KO mice. Error bars represent means + SEM of six individual mice. All *p* values were obtained using Student *t* test.

overexpression inhibited Treg conversion, we performed an analogous Treg conversion assay with anti-IFN- γ neutralizing Ab or an isotype control Ab. As shown in Fig. 12D, isotype control Ab did not affect Treg conversion. However, neutralization of IFN- γ restored the percentage of CD4⁺CD25⁺Foxp3⁺ cells to that observed with Cre⁻ DCs (Fig. 12D). Because microarray analysis also indicated overexpression of IFN- γ in MLN CD103⁺ DCs, we also examined the potential of MLN DCs to induce Treg differentiation. Similar to our results with BMDCs, we found that MLN DCs from DC-Tgfb2 KO mice were ineffective in converting naive T cells into Tregs (Fig. 12E), and elevated levels of IFN- γ were observed in the supernatants from Tgfb2 KO DC coculture (Fig. 12F). Addition of neutralizing Ab to IFN- γ rescued the conversion rate to levels close to that observed with control DCs (Fig. 12G).

In vitro-generated iTregs partially protect from autoimmunity in DC-Tgfb2 KO mice

Transfer of Tregs into young mice has been shown to prevent the development of autoimmune disease in mice (27). To determine whether adoptive transfer of CD4⁺CD25⁺Foxp3⁺ iTregs into DC-Tgfb2 KO mice can alleviate the autoimmune phenotype, polyclonal iTregs were generated *in vitro* by stimulating naive CD4⁺CD62L⁺ T cells with anti-CD3/CD28 in the presence of TGF- β , retinoic acid, and IL-2 for 4 d. These iTregs were then adoptively transferred *i.v.* into 2- to 3-wk-old Cre⁻ or DC-Tgfb2 KO mice. Control groups received PBS. The mice were monitored for 6 wk. Thirty-three percent of DC-Tgfb2 KO mice injected with PBS died during the course of the study, while no mortality was observed in DC-Tgfb2 KO mice transferred with iTregs (Fig. 13A). DC-Tgfb2 KO mice transferred with iTregs showed a significant decrease in the percentage of activated CD62L^{lo}CD44^{hi} CD4⁺ and CD8⁺ T cells in the spleen, compared with DC-Tgfb2 KO mice injected with PBS (Fig. 13B). Adoptive transfer of iTregs into DC-Tgfb2 KO mice significantly lowered TNF and IFN- γ expression in the proximal and distal colon, as compared with DC-Tgfb2 KO mice injected with PBS (Fig. 13C). Interestingly, iTreg transfer did not influence the development of gastritis, with no significant difference in TNF or IFN- γ expression in DC-Tgfb2 KO mice injected with iTregs or PBS (Fig. 13D). Similar results were obtained with other tissues including pancreas and liver (data not

shown), thus suggesting that the Treg-mediated suppression of autoimmune inflammation may be tissue-specific or may require Ag-specific Tregs and is not sufficient to completely rescue the phenotype of DC-Tgfb2 KO mice.

Discussion

DCs maintain a fine balance between immune activation to foreign Ags and tolerance to self-Ags. Under steady-state conditions, DCs mediate both clonal deletion of self-reactive T cells in the thymus and control of T cells specific responses to self- or harmless Ags in the periphery (29). These DCs are termed as tolerogenic DCs, but the signals that drive the tolerogenic pathways in these cells are just beginning to be understood (30). In this article, we provide conclusive *in vivo* evidence that TGF- β provides a signal that is essential to maintain the tolerogenic function of DCs, although in a manner not consistent with the reported *in vitro* studies. Loss of TGF- β signaling in DCs makes them more proinflammatory and less immunosuppressive, which in turn leads to the development of autoimmunity in mice.

The pathology of DC-Tgfb2 KO mice resembles that of Tgfb-null KO mice (Tgfb^{-/-}) (31), although with a delayed onset. Therefore, it is conceivable that apart from the impaired T cell homeostasis and enhanced T cell activation (32, 33), impaired DC function may also greatly contribute to disease severity in Tgfb^{-/-} mice. Although spontaneous upregulation of MHC class I and II were attributed to the observed autoimmune phenotype in Tgfb^{-/-} mice, we did not see any difference in the expression of MHCII or the costimulatory molecules CD80, CD86, and CD40 in DC-Tgfb2 KO mice, suggesting that loss of TGF- β signaling does not alter the Ag-presenting function of DCs as a direct effect. However, Tgfb2-deficient DCs were more proinflammatory in agreement with previous *in vitro* studies using BMDCs (3, 6). We observed increased TNF expression by splenic DCs and increased IFN- γ expression by MLN DCs. The difference in the expression of inflammatory cytokines by these two populations of DCs may be due to the differences in the DC lineage in these lymphoid organs. It is known that during autoimmune disease a subset of inflammatory DCs (TNF/inducible NO synthase-producing DCs) that produce TNF and iNOS populate the spleen. These DCs arise from monocyte precursors and can be cultured *in vitro* from BM precursors using GM-CSF and IL-4 (34). Indeed, we found in-

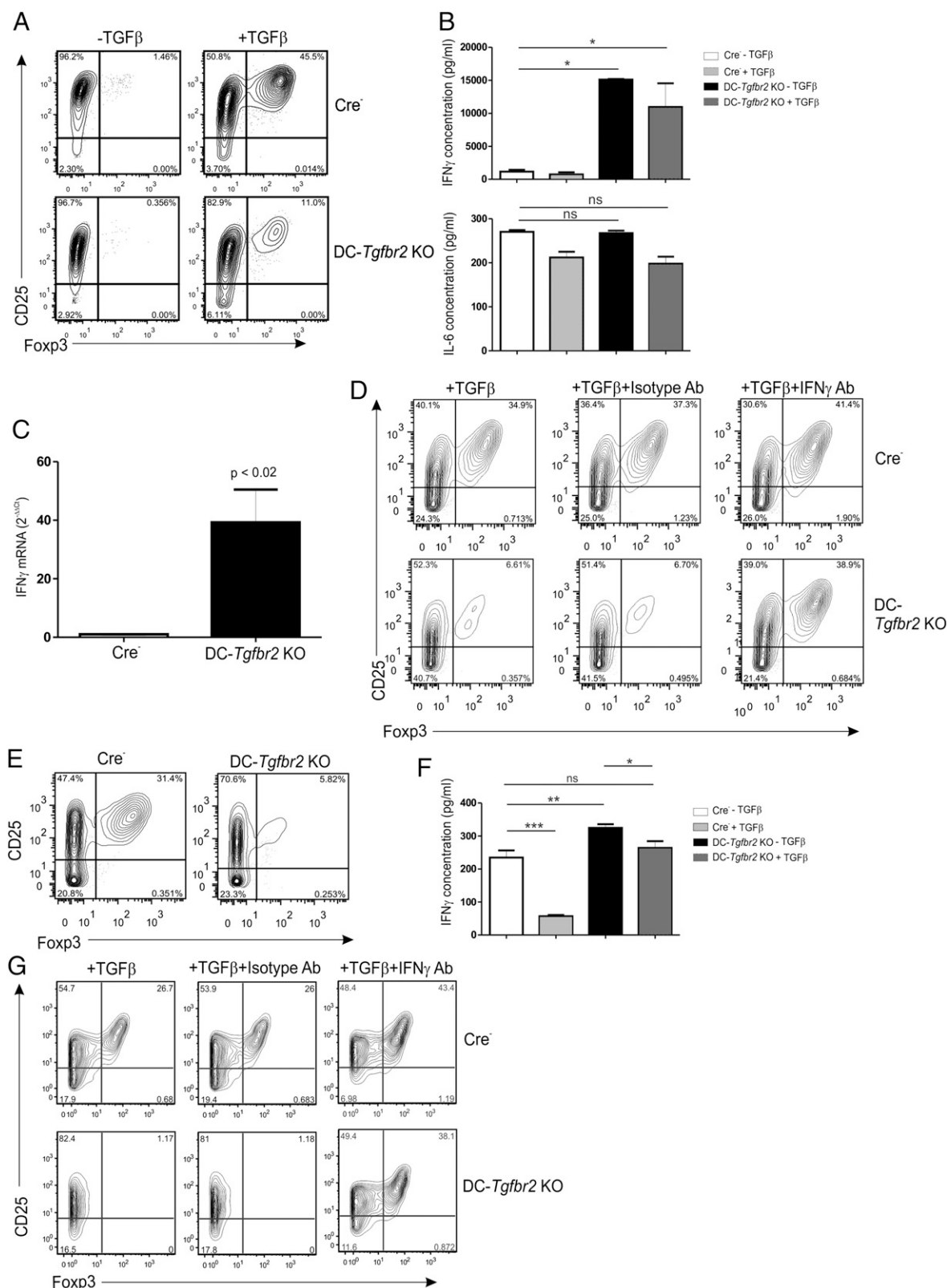


FIGURE 12. Increased IFN- γ production by *Tgfb2* KO DCs inhibits Treg differentiation. **(A)** Treg differentiation assay using Cre⁻ or DC-*Tgfb2* KO CD11c⁺ Flt3L BMDCs. OVA-pretreated DCs (500 μ g/ml) were cocultured with CD4⁺CD62L⁺ naive OT-II T cells (1:10) in the presence/absence of TGF- β (5 ng/ml) for 90 h. Percentage of CD4⁺CD25⁺Foxp3⁺ Tregs was determined by flow cytometry (representative of at least two experiments); **(B)** IFN- γ (top panel) and IL-6 (bottom panel) concentrations in the supernatants of Treg conversion assay as described in (A). Error bars represent means + SEM of triplicate samples. * p < 0.05 (one-way ANOVA with a Newman-Keuls post hoc test; data representative of at least two independent experiments); **(C)** *Ifng* mRNA in Flt3L CD11c⁺ BMDCs from Cre⁻ or DC-*Tgfb2* KO mice. Samples were normalized to TBP. Error bars represent SEM of triplicates. The p values were obtained using Student t test; **(D)** Treg conversion assay was performed using Cre⁻ (top panel) and DC-*Tgfb2* KO DCs (bottom panel) as described in (A) either alone (left panel) or with an isotype control Ab (middle panel) or anti-IFN- γ Ab (2 μ g/ml) (right panel); **(E)** CD25⁺Foxp3⁺ Tregs (left panel) obtained using CD11c⁺ MLN DCs from Cre⁻ or DC-*Tgfb2* KO mice. Protocol similar to that described in (A), (Figure legend continues)

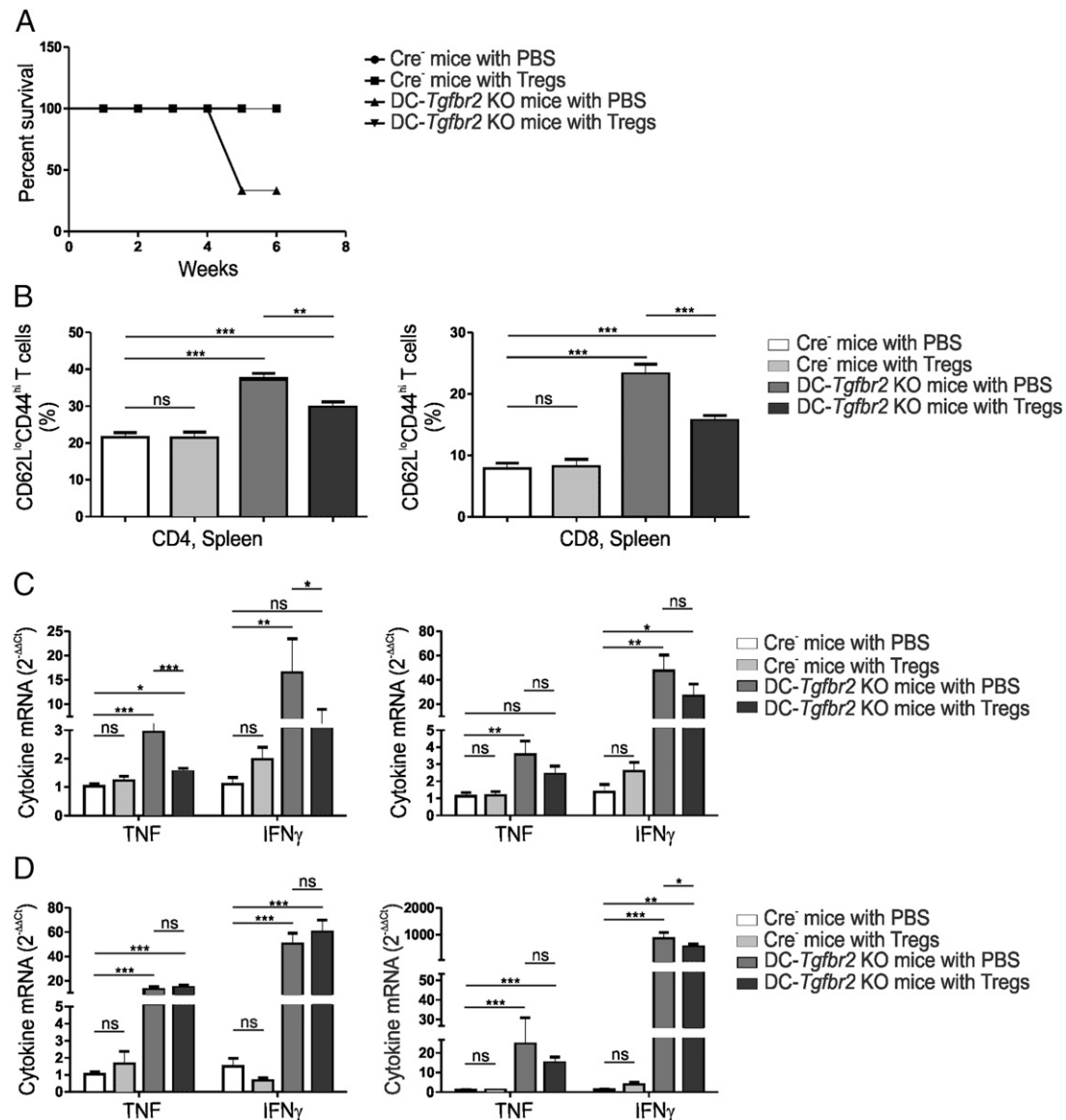


FIGURE 13. Adoptive transfer of Tregs partially rescues the autoimmune phenotype of DC-*Tgfb2* KO mice. **(A)** Survival curve of Cre⁻ or DC-*Tgfb2* KO mice injected with PBS or adoptively transferred at 2–3 wk of age with Foxp3⁺ iTregs (2×10^6 cells/mouse) generated as described in *Materials and Methods*; **(B)** percentage of CD4⁺ (left panel) and CD8⁺ (right panel) CD62L^{lo}CD44^{hi} T cells in the spleen of recipient mice at the end of the experiment described in (A); **(C)** cytokine mRNA expression in the proximal and distal colon of recipient mice as described in (A). Samples were normalized to TBP expression. Error bars represent means + SEM of six to seven individual mice; **(D)** cytokine mRNA expression in the forestomach and glandular stomach of recipient mice as described in (A). Error bars represent means + SEM of six to seven individual mice. * $p < 0.05$, ** $p < 0.01$, *** $p < 0.001$ (one-way ANOVA with a Newman–Keuls post hoc test).

creased TNF production in BMDCs differentiated using GM-CSF and IL-4, and these DCs were able to exacerbate T cell-mediated colitis. MLN CD103⁺ DCs (and CD103⁻ DC; data not shown), as well as Flt3L-differentiated BMDC from DC-*Tgfb2* KO, showed elevated IFN- γ expression without additional stimulation. Interestingly, microarray analysis of splenic DCs from DC-*Tgfb2* KO mice showed a clear IFN- γ signature response, although expression of IFN- γ itself was not elevated. Similarly, splenic DCs from CD11c^{dnR} mice did not produce IFN- γ even after stimulation with IL-12 and IL-18 (15). These two observations suggest differences

in IFN- γ induction in the splenic and mucosal/LN DC lineages and/or that DCs migrating to the spleen are primed by IFN- γ at the mucosal/parenchymal sites. This is also consistent with the fact that CD103⁺ DCs produce higher levels of active TGF- β (35), which may act in an autocrine or paracrine manner to suppress IFN- γ expression, both in CD103⁺ and CD103⁻ DCs.

Although TGF- β has been shown to induce expression of IDO in DCs (9, 36), we did not find any significant differences in the expression of IDO in either splenic DCs or MLN CD103⁺ DCs. Expression and activity of IDO protein in *Tgfb2* KO mucosal

except that DCs were cocultured with T cells (1:2) in the presence of 1 mg/ml OVA; **(F)** IFN- γ expression (ELISA) in the supernatants of Treg conversion assay with MLN DCs. * $p < 0.05$, ** $p < 0.01$, *** $p < 0.001$ (one-way ANOVA with Newman–Keuls post hoc test). **(G)** Treg conversion assay was performed using Cre⁻ (top panel) and DC-*Tgfb2* KO DCs (bottom panel) as described in (E) (DC/T cell ratio, 1:10) either alone (left panel), with an isotype control (middle panel), or anti-IFN- γ neutralizing Ab (2 μ g/ml) (right panel). Representative data from one of three repetitions is shown.

DCs remain to be investigated. Lack of detectable changes in IDO expression in MLN or splenic DCs may represent the net effect of the absence or reduction of stimulatory TGF- β signaling and compensatory autocrine effects of elevated IFN- γ , which is known to induce IDO expression (37). In pDCs, TGF- β also controls nonenzymatic cell signaling functions of IDO without affecting its expression levels (10). It is therefore plausible that this pathway may also be affected, thus leading to the loss of regulatory phenotype in pDCs, a response skewed toward the canonical NF- κ B pathway, more inflammatory state, and ultimately loss of tolerance in DC-*Tgfb2* KO mice.

Immunosuppressive Tregs control T cell activation and prevent the development of autoimmune disease. Expression of Foxp3 in secondary lymphoid CD4⁺ T cells was significantly decreased, along with a decrease in the frequency of CD4⁺CD25⁺Foxp3⁺ Tregs in DC-*Tgfb2* KO mice. Moreover, among the CD4⁺Foxp3⁺ T cells, we observed a dramatic increase in the proportion of CD4⁺CD25⁺Foxp3⁺ T cells, a population also reported recently in patients with systemic lupus erythematosus (38, 39) and relapsing patients with multiple sclerosis (40). The immunosuppressive potential of CD4⁺CD25⁺Foxp3⁺ Tregs is not entirely clear. Functional analyses of this population from SLE patients revealed a partial loss of function (39, 41). Zelenay et al. (42) showed that CD4⁺CD25⁺Foxp3⁺ T cells constitute a reservoir of committed Tregs that regain CD25 expression upon homeostatic proliferation in a lymphopenic host. However, the same group showed that Tregs identified as the CD45RB^{lo}CD25⁺ subset failed to show suppressive function in vitro when freshly isolated from mice (42). It has also been shown that Tregs with attenuated Foxp3 expression have lower levels of CD25 and that these cells have a tendency to convert to Th2 type cells (43). On the basis of these studies, it is highly likely that the CD4⁺CD25⁺Foxp3⁺ T cells in DC-*Tgfb2* KO mice are less immunosuppressive thereby contributing to the autoimmune pathology. Such alterations in Treg homeostasis and spontaneous autoimmunity were not observed in CD11c^{dnR} mice, suggesting that residual TGF- β signaling in DCs may have been sufficient to maintain self-tolerance under basal conditions and that the consequences of impaired TGF- β signaling in DCs may represent a continuum depending on the degree of suppression. Future studies with DC-*Tgfb2* KO crossed with Foxp3-RFP knockin mice should further clarify the nature and function of the CD4⁺CD25⁺Foxp3⁺ T cells.

We have also demonstrated that in vitro, DC-mediated Ag-specific Treg conversion is impaired because of elevated production of IFN- γ by *Tgfb2* KO DCs. However, we did not observe the expansion of the CD4⁺CD25⁺Foxp3⁺ population as we did in vivo. Therefore, the mechanisms leading to the potential loss of function of Tregs in DC-*Tgfb2* KO mice remain unclear. Bidirectional DC-Treg interactions are required to maintain immunological tolerance (44). DCs induce Treg differentiation and proliferation through Ag-dependent and -independent interactions but in a cell-cell contact- and IL-2-dependent mechanism (45). However, the suppressive function of the expanded Tregs may still require additional signals that remain unidentified. Adoptive transfer of in vitro-generated polyclonal Foxp3⁺ iTregs into young DC-*Tgfb2* KO mice prevented early mortality and partially rescued the autoimmune phenotype with significant reduction in the proportion of activated T cells and protection from colitis. It did not, however, protect from gastritis, pancreatitis, or hepatitis. Although the optimal timing of transfer and lifespan of the injected Tregs may be debatable, loss of their immunosuppressive function in vivo in DC-*Tgfb2* KO mice cannot be ruled out. In contrast, iTregs are generally thought to suppress immune responses to environmental, food allergens, and commensal microbiota, whereas

natural Tregs prevent autoimmunity by raising the threshold for activation of immune response to self-Ags (46). Consistent with our observations, non-Ag-specific iTregs have been shown to be protective in mouse models of colitis (46). In contrast, natural Tregs are selected in the thymus through MHCII-dependent TCR interactions and may mediate suppression in an Ag-specific manner. Ag-specific Tregs were required to prevent autoimmune gastritis in mice (47), which may explain persistent gastritis in our Treg rescue model.

This novel mouse model with DC-specific *Tgfb2* deletion highlights the critical importance of TGF- β signaling in DCs in the maintenance of immune homeostasis and in the prevention of autoimmunity. However, these functions may be independent of the previously ascribed TGF- β control of Ag presentation and costimulation. Although a mechanistic relationship between TGF- β signaling in DCs and Foxp3⁺ Treg responses still remains to be elucidated in detail, the phenotype of our novel mouse model can be exploited to advance our understanding of the pathogenesis of complex autoimmune disorders, including the in vivo expansion and function of CD25⁺Foxp3⁺ Tregs.

Acknowledgments

We thank Drs. Tom Doetschman and Nicolas Larmonier for helpful discussions, Dr. David Besselsen for help with pathological evaluation, Darya Alizadeh and Paula Campbell for assistance with flow cytometry and flow sorting, and Dr. Vijay Radhakrishnan for proofreading help.

Disclosures

The authors have no financial conflicts of interest.

References

- Li, M. O., Y. Y. Wan, S. Sanjabi, A. K. Robertson, and R. A. Flavell. 2006. Transforming growth factor-beta regulation of immune responses. *Annu. Rev. Immunol.* 24: 99–146.
- Grauer, O., P. Pöschl, A. Lohmeier, G. J. Adema, and U. Bogdahn. 2007. Toll-like receptor triggered dendritic cell maturation and IL-12 secretion are necessary to overcome T-cell inhibition by glioma-associated TGF- β 2. *J. Neurooncol.* 82: 151–161.
- Geissmann, F., P. Revy, A. Regnault, Y. Lepelletier, M. Dy, N. Brousse, S. Amigorena, O. Hermine, and A. Durandy. 1999. TGF- β 1 prevents the noncognate maturation of human dendritic Langerhans cells. *J. Immunol.* 162: 4567–4575.
- Ronger-Savle, S., J. Valladeau, A. Claudy, D. Schmitt, J. Peguet-Navarro, C. Dezutter-Dambuyant, L. Thomas, and D. Jullien. 2005. TGF β inhibits CD1d expression on dendritic cells. *J. Invest. Dermatol.* 124: 116–118.
- Yamaguchi, Y., H. Tsumura, M. Miwa, and K. Inaba. 1997. Contrasting effects of TGF- β 1 and TNF- α on the development of dendritic cells from progenitors in mouse bone marrow. *Stem Cells* 15: 144–153.
- Siddiqui, K. R., S. Laffont, and F. Powrie. 2010. E-cadherin marks a subset of inflammatory dendritic cells that promote T cell-mediated colitis. *Immunity* 32: 557–567.
- Ogata, M., Y. Zhang, Y. Wang, M. Itakura, Y. Y. Zhang, A. Harada, S. Hashimoto, and K. Matsushima. 1999. Chemotactic response toward chemokines and its regulation by transforming growth factor- β 1 of murine bone marrow hematopoietic progenitor cell-derived different subset of dendritic cells. *Blood* 93: 3225–3232.
- Sato, K., H. Kawasaki, H. Nagayama, M. Enomoto, C. Morimoto, K. Tadokoro, T. Fuji, and T. A. Takahashi. 2000. TGF- β 1 reciprocally controls chemotaxis of human peripheral blood monocyte-derived dendritic cells via chemokine receptors. *J. Immunol.* 164: 2285–2295.
- Belladonna, M. L., C. Volpi, R. Bianchi, C. Vacca, C. Orabona, M. T. Pallotta, L. Boon, S. Gizzi, M. C. Fioretti, U. Grohmann, and P. Puccetti. 2008. Cutting edge: autocrine TGF- β sustains default tolerogenesis by IDO-competent dendritic cells. *J. Immunol.* 181: 5194–5198.
- Pallotta, M. T., C. Orabona, C. Volpi, C. Vacca, M. L. Belladonna, R. Bianchi, G. Servillo, C. Brunacci, M. Calvitti, S. Biccato, et al. 2011. Indoleamine 2,3-dioxygenase is a signaling protein in long-term tolerance by dendritic cells. *Nat. Immunol.* 12: 870–878.
- Brenner, O., D. Levanon, V. Negreanu, O. Golubkov, O. Fainaru, E. Woolf, and Y. Groner. 2004. Loss of Runx3 function in leukocytes is associated with spontaneously developed colitis and gastric mucosal hyperplasia. *Proc. Natl. Acad. Sci. USA* 101: 16016–16021.
- Fainaru, O., E. Woolf, J. Lotem, M. Yarmus, O. Brenner, D. Goldenberg, V. Negreanu, Y. Bernstein, D. Levanon, S. Jung, and Y. Groner. 2004. Runx3 regulates mouse TGF- β -mediated dendritic cell function and its absence results in airway inflammation. *EMBO J.* 23: 969–979.

13. Laouar, Y., T. Town, D. Jeng, E. Tran, Y. Wan, V. K. Kuchroo, and R. A. Flavell. 2008. TGF- β signaling in dendritic cells is a prerequisite for the control of autoimmune encephalomyelitis. *Proc. Natl. Acad. Sci. USA* 105: 10865–10870.
14. Sanjabi, S., and R. A. Flavell. 2010. Overcoming the hurdles in using mouse genetic models that block TGF- β signaling. *J. Immunol. Methods* 353: 111–114.
15. Laouar, Y., F. S. Sutterwala, L. Gorelik, and R. A. Flavell. 2005. Transforming growth factor- β controls T helper type 1 cell development through regulation of natural killer cell interferon- γ . *Nat. Immunol.* 6: 600–607.
16. Boomersshine, C. S., A. Chamberlain, P. Kendall, A. R. Afshar-Sharif, H. Huang, M. K. Washington, W. E. Lawson, J. W. Thomas, T. S. Blackwell, and N. A. Bhowmick. 2009. Autoimmune pancreatitis results from loss of TGF β signalling in S100A4-positive dendritic cells. *Gut* 58: 1267–1274.
17. Shevach, E. M. 2009. Mechanisms of foxp3⁺ T regulatory cell-mediated suppression. *Immunity* 30: 636–645.
18. Darrasse-Jèze, G., S. Deroubaix, H. Mouquet, G. D. Vitoria, T. Eisenreich, K. H. Yao, R. F. Masilamani, M. L. Dustin, A. Rudensky, K. Liu, and M. C. Nussenzweig. 2009. Feedback control of regulatory T cell homeostasis by dendritic cells in vivo. *J. Exp. Med.* 206: 1853–1862.
19. Chen, W., W. Jin, N. Hardegen, K. J. Lei, L. Li, N. Marinos, G. McGrady, and S. M. Wahl. 2003. Conversion of peripheral CD4⁺CD25⁺ naive T cells to CD4⁺CD25⁺ regulatory T cells by TGF- β induction of transcription factor Foxp3. *J. Exp. Med.* 198: 1875–1886.
20. Caton, M. L., M. R. Smith-Raska, and B. Reizis. 2007. Notch-RBP-J signaling controls the homeostasis of CD8⁺ dendritic cells in the spleen. *J. Exp. Med.* 204: 1653–1664.
21. Chytil, A., M. A. Magnuson, C. V. Wright, and H. L. Moses. 2002. Conditional inactivation of the TGF- β type II receptor using Cre:Lox. *Genesis* 32: 73–75.
22. Mombaerts, P., J. Iacomini, R. S. Johnson, K. Herrup, S. Tonegawa, and V. E. Papaioannou. 1992. RAG-1-deficient mice have no mature B and T lymphocytes. *Cell* 68: 869–877.
23. Xu, Y., Y. Zhan, A. M. Lew, S. H. Naik, and M. H. Kershaw. 2007. Differential development of murine dendritic cells by GM-CSF versus Flt3 ligand has implications for inflammation and trafficking. *J. Immunol.* 179: 7577–7584.
24. Ohnmacht, C., A. Pullner, S. B. King, I. Drexler, S. Meier, T. Brocker, and D. Voehringer. 2009. Constitutive ablation of dendritic cells breaks self-tolerance of CD4 T cells and results in spontaneous fatal autoimmunity. *J. Exp. Med.* 206: 549–559.
25. Hadeiba, H., T. Sato, A. Habtezion, C. Oderup, J. Pan, and E. C. Butcher. 2008. CCR9 expression defines tolerogenic plasmacytoid dendritic cells able to suppress acute graft-versus-host disease. *Nat. Immunol.* 9: 1253–1260.
26. Hakim, F. T., and R. E. Gress. 2007. Thymic involution: implications for self-tolerance. *Methods Mol. Biol.* 380: 377–390.
27. Sakaguchi, S., T. Yamaguchi, T. Nomura, and M. Ono. 2008. Regulatory T cells and immune tolerance. *Cell* 133: 775–787.
28. Yamazaki, S., A. J. Bonito, R. Spisek, M. Dhodapkar, K. Inaba, and R. M. Steinman. 2007. Dendritic cells are specialized accessory cells along with TGF- β for the differentiation of Foxp3⁺CD4⁺ regulatory T cells from peripheral Foxp3 precursors. *Blood* 110: 4293–4302.
29. Steinman, R. M., D. Hawiger, and M. C. Nussenzweig. 2003. Tolerogenic dendritic cells. *Annu. Rev. Immunol.* 21: 685–711.
30. Manicassamy, S., and B. Pulendran. 2011. Dendritic cell control of tolerogenic responses. *Immunol. Rev.* 241: 206–227.
31. Shull, M. M., I. Ormsby, A. B. Kier, S. Pawlowski, R. J. Diebold, M. Yin, R. Allen, C. Sidman, G. Proetzel, D. Calvin, et al. 1992. Targeted disruption of the mouse transforming growth factor- β 1 gene results in multifocal inflammatory disease. *Nature* 359: 693–699.
32. Li, M. O., S. Sanjabi, and R. A. Flavell. 2006. Transforming growth factor- β controls development, homeostasis, and tolerance of T cells by regulatory T cell-dependent and -independent mechanisms. *Immunity* 25: 455–471.
33. Marie, J. C., D. Liggitt, and A. Y. Rudensky. 2006. Cellular mechanisms of fatal early-onset autoimmunity in mice with the T cell-specific targeting of transforming growth factor- β receptor. *Immunity* 25: 441–454.
34. Shortman, K., and S. H. Naik. 2007. Steady-state and inflammatory dendritic-cell development. *Nat. Rev. Immunol.* 7: 19–30.
35. Coombes, J. L., K. R. Siddiqui, C. V. Arancibia-Cárcamo, J. Hall, C. M. Sun, Y. Belkaid, and F. Powrie. 2007. A functionally specialized population of mucosal CD103⁺ DCs induces Foxp3⁺ regulatory T cells via a TGF- β and retinoic acid-dependent mechanism. *J. Exp. Med.* 204: 1757–1764.
36. Belladonna, M. L., C. Orabona, U. Grohmann, and P. Puccetti. 2009. TGF- β and kynurenines as the key to infectious tolerance. *Trends Mol. Med.* 15: 41–49.
37. Mellor, A. L., and D. H. Munn. 2004. IDO expression by dendritic cells: tolerance and tryptophan catabolism. *Nat. Rev. Immunol.* 4: 762–774.
38. Yang, H. X., W. Zhang, L. D. Zhao, Y. Li, F. C. Zhang, F. L. Tang, W. He, and X. Zhang. 2009. Are CD4⁺CD25⁺Foxp3⁺ cells in untreated new-onset lupus patients regulatory T cells? *Arthritis Res. Ther.* 11: R153.
39. Bonelli, M., A. Savitskaya, C. W. Steiner, E. Rath, J. S. Smolen, and C. Scheinecker. 2009. Phenotypic and functional analysis of CD4⁺CD25⁺Foxp3⁺ T cells in patients with systemic lupus erythematosus. *J. Immunol.* 182: 1689–1695.
40. Fransson, M., J. Burman, C. Lindqvist, C. Atterby, J. Fagius, and A. Loskog. 2010. T regulatory cells lacking CD25 are increased in MS during relapse. *Autoimmunity* 43: 590–597.
41. Horwitz, D. A. 2010. Identity of mysterious CD4⁺CD25⁺Foxp3⁺ cells in SLE. *Arthritis Res. Ther.* 12: 101.
42. Zelenay, S., T. Lopes-Carvalho, I. Caramalho, M. F. Moraes-Fontes, M. Rebelo, and J. Demengeot. 2005. Foxp3⁺CD25⁺ CD4 T cells constitute a reservoir of committed regulatory cells that regain CD25 expression upon homeostatic expansion. *Proc. Natl. Acad. Sci. USA* 102: 4091–4096.
43. Wan, Y. Y., and R. A. Flavell. 2007. Regulatory T-cell functions are subverted and converted owing to attenuated Foxp3 expression. *Nature* 445: 766–770.
44. Lange, C., M. Dür, H. Doster, A. Melms, and F. Bischof. 2007. Dendritic cell-regulatory T-cell interactions control self-directed immunity. *Immunol. Cell Biol.* 85: 575–581.
45. Zou, T., A. J. Caton, G. A. Koretzky, and T. Kambayashi. 2010. Dendritic cells induce regulatory T cell proliferation through antigen-dependent and -independent interactions. *J. Immunol.* 185: 2790–2799.
46. Curotto de Lafaille, M. A., and J. J. Lafaille. 2009. Natural and adaptive foxp3⁺ regulatory T cells: more of the same or a division of labor? *Immunity* 30: 626–635.
47. Nguyen, T. L., N. L. Sullivan, M. Ebel, R. M. Teague, and R. J. DiPaolo. 2011. Antigen-specific TGF- β -induced regulatory T cells secrete chemokines, regulate T cell trafficking, and suppress ongoing autoimmunity. *J. Immunol.* 187: 1745–1753.